2D SEISMIC INTERPRETATION AND PETROPHYSICAL ANALYSIS OF BALKASSAR OIL FIELD, UPPER INDUS BASIN, PAKISTAN

BY

SAJJAD ALI

ZAIR KHAN

HAMMAD MUSTAFA

DEPARTMENT OF EARTH AND ENVIRONMENTAL SCIENCES BAHRIA UNIVERSITY, ISLAMABAD

2021

2D SEISMIC INTERPRETATION AND PETROPHYSICAL ANALYSIS OF BALKASSAR OIL FIELD, UPPER INDUS BASIN, PAKISTAN

A thesis submitted to Bahria University, Islamabad in partial fulfillment of the requirement for the degree of BS in Geophysics

SAJJAD ALI

ZAIR KHAN

HAMMAD MUSTAFA

DEPARTMENT OF EARTH AND ENVIRONMENTAL SCIENCES

BAHRIA UNIVERSITY, ISLAMABAD

2021

ABSTRACT

The Balkassar oilfield is one of the major hydrocarbon producing field in Potwar Plateau, Upper Indus Basin Pakistan. This field has been producing both oil and gas from tectonically fractured carbonates deposits of Eocene age. Using six seismic lines and one well data we delineate the hydrocarbon potential of the Balkassar area by 2D seismic interpretation and petrophysical analysis that has been carried out and is represented in the current study. Most of the structural traps in Balkassar area are due to the oldest salt range formation in which the salt diapirism is responsible for the formation of these traps. The direction of deformation is in north-west/south-east. The main productive reservoir formations of Balkassar area are Chorgali Formation and Sakessar Limestone which are being charged by shales of Patala Formation of Paleocene age. Identification of formation is done through seismic section based on time-depth chart and well tops. The major thrust and back thrust are a structural trap bounded by the anticline and the clays of Murree Formation act as a seal rock.

ACKNOWLEDGMENTS

We are thankful to Almighty Allah, the most beneficent and the most merciful, for His boundless blessings with which we qualified to pursue this thesis despite living in one of the most unprecedented times in our history. Working on a thesis during COVID-19 was a unique experience with several challenges.

We are highly obliged to our supervisor Mr. Muhammad Raiees Amjad, Assistant Professor, Department of Earth and Environmental Sciences, Bahria University Islamabad, for his guidance, cooperation, precious time, and moral support to complete this dissertation with dedication. We are also thankful to Ms. Urooj Shakir, Senior Assistant Professor for her guidance throughout our final project.

Thanks, are also extended to the Head of Department, Earth & Environmental Sciences, Bahria University, Islamabad.

CONTENTS

CHAPTER 3
SEISMIC DATA INTERPRETATION

CHAPTER 4
PETROPHYSICAL ANALYSIS

FIGURES

Page

TABLES

Page

CHAPTER 1

INTRODUCTION

1.1 General introduction

Mighty earth contains surplus amounts of valuable treasures like oil, gas, mineral and gemstones for mankind. The earth is a body that involves plenty of continuous processes like tectonism, evaluation of magma and formation of various rock types. The curiosity in the man has intrigued him to explore the earth more and more in terms of geography, geology, geophysics, topology, climatology, and various other ways of understanding what is laying under, upon and over it (Milsom and Eriksen, 2011).

There are different branches of physics including geophysics, which focuses mainly on indirect observation of structures and processes laying underneath the earth. Understanding of these processes and structures is made possible by using different geophysical techniques like seismic method, magnetic method, resistivity method, gravity method, electric resistivity method, well logging method and radioactive method. The seismic method is an advance geophysical technique used by geophysicists to explore hydrocarbons and evaluate the subsurface lithologies and structures (Milsom and Eriksen, 2011).

Using seismic survey, we acquire data like seismic sections from subsurface by using parameters such as arrival time, Polarity, and phase of traces (reflectors and refractors), when the seismic waves generate from the seismic source (vibroseis) and when they come back after striking from subsurface then we interpret the seismic section and evaluate the structures, lithology, and hydrocarbon potential at a given depth. Seismic interpretation involves structural and stratigraphic interpretation that would be discussed in detailed in the 3rd chapter of this document. Authentication of seismic interpretation will lead to the drilling of successful well (Badley 1985).

Petrophysical analysis of any area performed by data like well logs along with seismic interpretation would determine the rock parameters such as porosity, permeability, rock saturation (water, hydrocarbons) density and resistivity of rock. These parameters help Petro-physicists and geophysicists for better reservoir characterization. Evaluation of

reservoir character helps us in identifying our prospects and plays, the probability and possibility of achievements and in the making of future-plans for the drilling wells (Archie 1992).

1.2 Introduction of study area

The area which lies in the north of salt range is called Potwar plateau due to its relatively constant tectonic evaluation and presence of abundant drainage area of soan river. Potwar plateau is roughly defined by the river Indus and Jhelum to the west and east respectively while Kala Chitta Margalla hill ranges to the north and the salt range to the south. This plateau is largely covered by the Siwalik's sequence, thought at places upper Eocene shales and limestones crop out locally enfolded inliers. Its northern part known as north Potwar deformed zone (NPDZ) is more intensely deformed. It is characterized by east west, tight, and complex fold, over-turned to the south and sheared by steep angle faults. The north Potwar deformed Potwar zone bound south by broad Soan syncline, with a gently northward dipping southern flank along the salt range and a steeply dipping northern limb along north Potwar zone. Faulting of anticlines is rare (Pennock et al. 1989). Integration of seismic reflections, gravity and drilled holes data with surface geology shows that the salt range and Potwar are underlain by a general 1 to 4 degrees northward dipping basement with an upward convexity and reversed by northward dipping normal fault and traversed by north dipping normal faults. There are two major strike slip faults that bound the plateau from east and west that are Jhelum and kalabagh respectively, in the north by MBT and in the south by salt range thrust that is been shown in the figure 1.1. Potwar sub basin is one of the oldest oil-province of the world (Kazmi and Jan 1977).

Image of sub surface provides a structural style and stratigraphic variations of a basin. Due to the presence of decollement at different levels, the Potwar sub-basin's surface features do not reflect the sub-surface structure variations. In such cases, it is necessary to integrate seismic data and make perfect geological model. The seismic trainsets along with geological transposition exhibit distinct domain from south to north and eastern and western part of the basin. Due to the compressional forces the occurrence of effective fracture system in various Eocene carbonate deposits that act as a reservoir rock in this basin (Iqbal & Ali, 2001).

1.3 Location of study area

Balkassar, an exclusive development and production lease of Pakistan oil fields limited, was discovered in 1945 by Attock oil company. It is situated about 112 km South-East of Islamabad which is shown in figure 1.2. Balkassar lies in central part of Potwar sub basin which is a part of Himalayan foreland fold and thrust belt. This structure is located on the southern limb of Soan syncline.

The seismic reflection data was acquired by OGDCL in 1980 and processed by OGDCL in 1981. The status of the well is plugged and abandoned. The client for this survey was OXY (Pakistan). Currently, Balkassar field was producing about 750 barrels oil per day from Eocene carbonate rocks. OXY require the lease to evaluate the deeper potential below 1982 meters sub-sea. The coordinates of Balkassar Oxy-1 lie at the latitude 32° 56’ 38.8” N and the longitude 72°39’52.5” E.

Figure 1. 1 Location of Study Area(https://biogeo.ucdavis.edu/data/diva/adm/PAK_adm.zip)

1.4 Objectives of study area

1. To delineate subsurface structure present at the area using 2D seismic data.
2. Evaluation of reservoir rocks through petrophysical analysis.

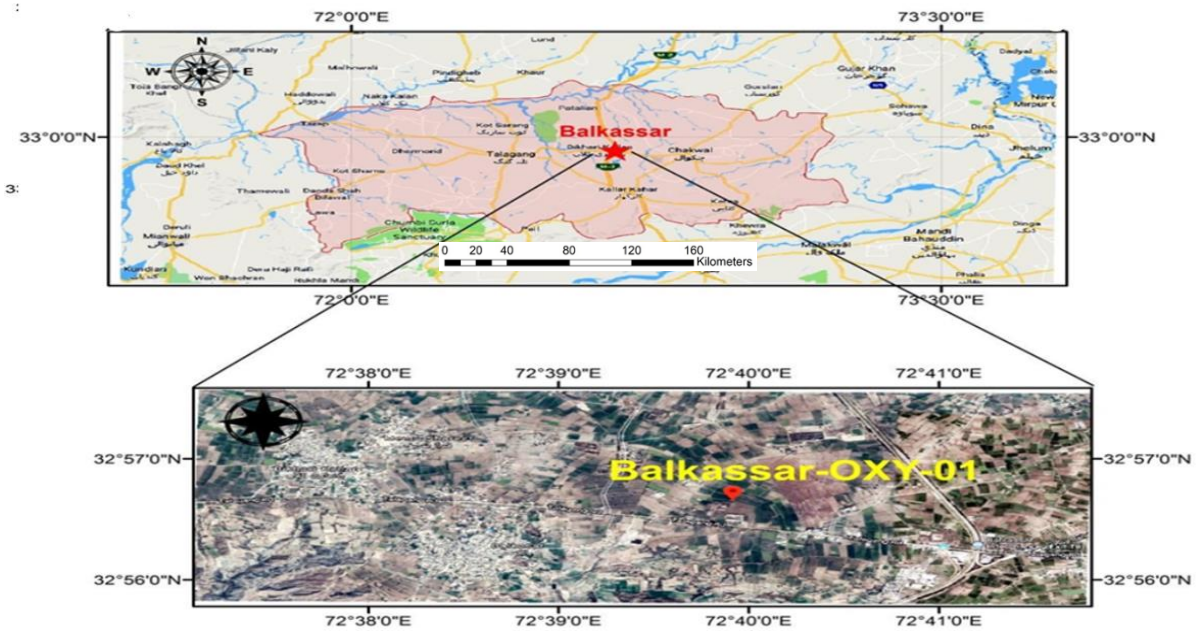

Figure 1.1. Location of study area.

1.5 Data acquired

We acquired our data from LMKR after it was approved from DGPC and consisted of:

Table 1.1 Shows seismic lines.

Sr. No.	Seismic line	Company	Type	Shooting direction
1.	SOX-PBJ-1	OGDCL	Dip line	NW-SE
2.	SOX-PBJ-4	OGDCL	Dip line	NW-SE
3.	SOX-PBJ-6	OGDCL	Dip line	NW-SE
4.	SOX-PBJ-8	OGDCL	Strike line	NE-SW
5.	SOX-PBJ-9	OGDCL	Strike line	NE-SW
6.	SOX-PBJ-10	OGDCL	Strike line	NE-SW

1. Well, tops.
2. Well log data of Balkassar Oxy-01.
3. Navigation file.

1.5.1 Well data

Well logs of Balkassar Oxy-01 include:

1. Caliper log
2. Neutron log
3. Gamma ray log
4. Spontaneous potential log
5. Resistivity log
6. Sonic log

1.5.2 Seismic data

The seismic data consists of three strike lines and the three dip lines and their details are shown in the table 1.1.

1.6 Methodology

Methodology of this study involves seismic interpretation and petrophysical analysis. The methodology of these are shown in figure 1.2 and 1.3 respectively.

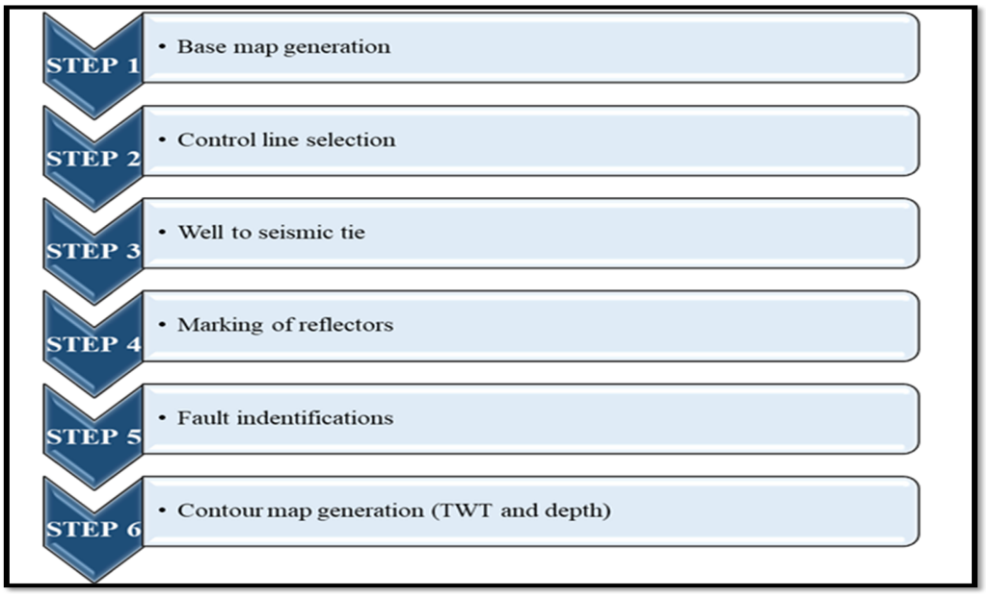

Figure 1.2. Workflow of seismic interpretation.

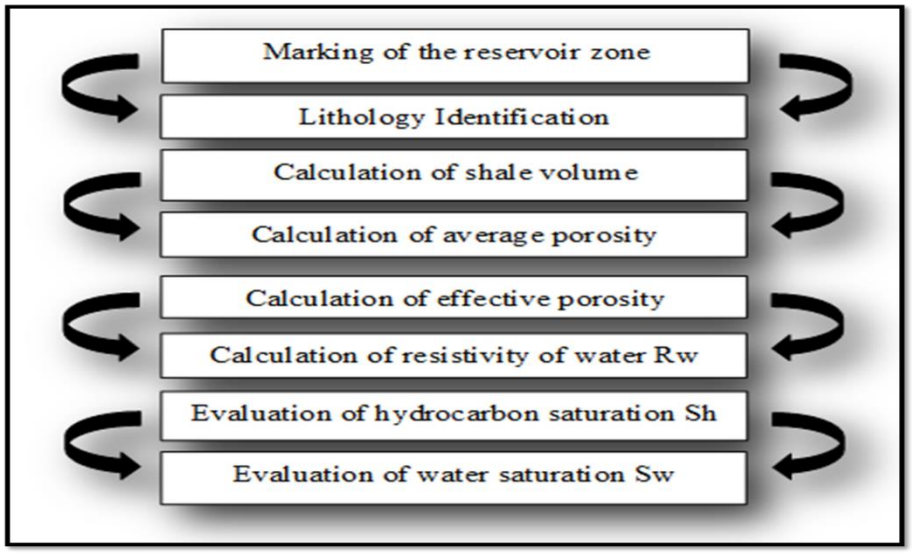

Figure 1.3.Workflow of petrophysical analysis

CHAPTER 2

GEOLOGY AND TECTONICS

2.1 Introduction

Pakistan has been geologically well known for several decades for its great mountains, extensive glaciers, devastating earthquakes, exotic and prolific Neogene vertebrate fauna, chromite bearing ophiolites, Pre-Cambrian, and Paleozoic succession of salt range, the abundant Oro-clinal flexures and enigmatic syntaxes in its mountain ranges, deep gorges and canyons that highlight the antecedent drainage. These geologic features have been largely revealed by the reconnaissance surveys of earlier pioneers who explored the vast areas despite a lack of proper topographic maps and absence of roads and communication system. In an area of 800,000 km squares the geological setting of Pakistan is rare and match less due to the presence of critical tectonic junctions of plates and micro plates. The Indo-Pak subcontinent separated from the mother Gondwana land about 130 million years ago (Jonson et al., 1976).

Pakistan lies on Eurasian and Indian Plate where the Indian Plate slid in the Northward direction that has been estimated between 130 and180 million years at the rate of 3-5cm per year. According to Patriat and Achache (1984) before 50 million years ago, this rate of movement varied between 15-25 cm per year. The movement was facilitated by the transform faulting and extensive extrusion of Deccan trap basalts occurred between 65-60 million years ago (Duncan et al., 1988), during the fast northward drift towards India. The collision occurred between the Eurasian plate and the Indian plate approximately 55 million years ago, due to this collision typical plateau and Himalayan-mountain ranges have formed. Because of continent-continent collision, it is still active today which leads to continuous erosion, uplifting and sediment deposition (Kazmi and Jan,1997).

2.2 General Geology and tectonics of study area

Potwar sub basin is structurally bounded by the MBT to the north, Salt Range to the south, Kalabagh to the west and the Jhelum fault to the east. The structures formed in our study area are highly faulted and tightly folded. Back thrust and the major thrust bound the anticlinal features. Balkassar oilfield is a platform area having duplex geometry that is

overlain by passive roof complex sequence of younger Siwaliks (Shakir et al.,2020). The pop-up geometry and the anticlinal structures indicate that our study area is lying in a compressional regime and due to the presence of salt in the subsurface, act as a decollement that is responsible for the pop-up geometry and anticlinal, synclinal, and normal faulting features. The structure is bounded by the MBT in strike direction. Some orthogonal faults are also present that are responsible of lateral barriers to the hydrocarbon flow during production (Zaman et al., 1996, Mehmood et al., 2016). Main structure features of Potwar sub-basin areas are:

1. Tawan anticline
2. Domeli thrust
3. Adhi-gungril anticline
4. Chak-naurang anticline
5. Soan syncline
6. Jhelum fault and Kalabagh fault
7. Salt range thrust
8. Salt range

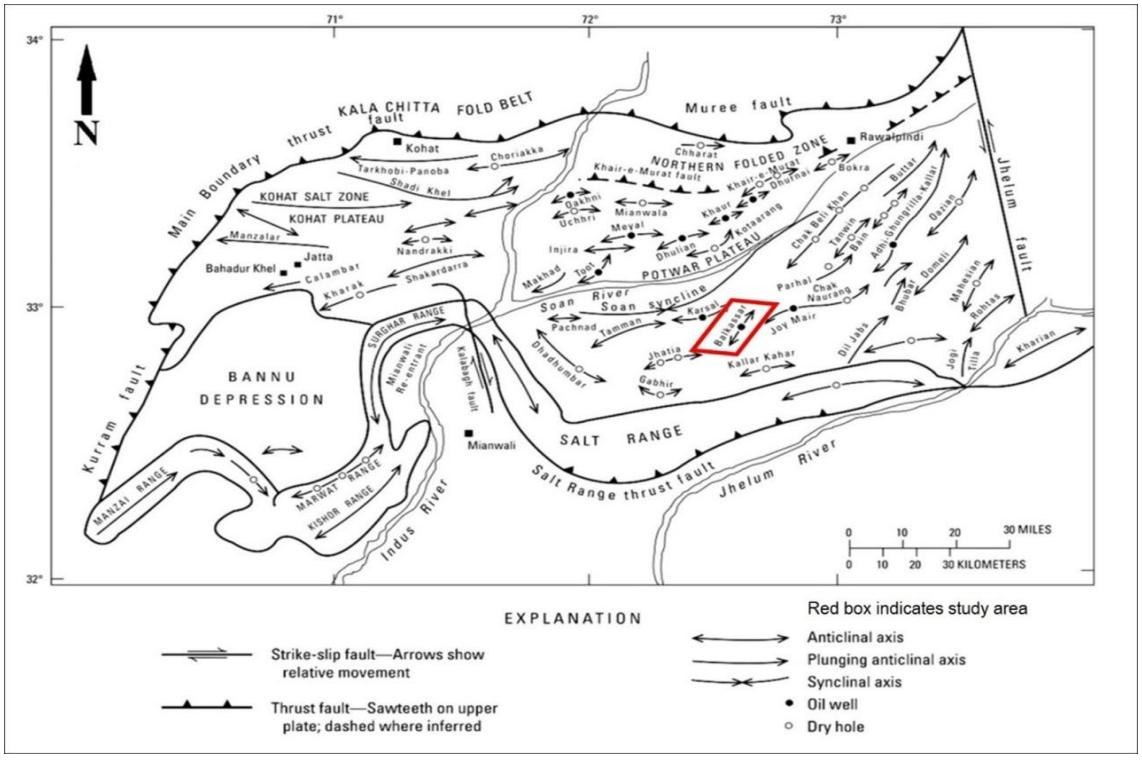

Figure 2.1. Tectonic map of Upper Indus basin highlighting the study area Balkassar (Warwick, P.D 2004)

2.3 Sedimentary basin

Sedimentary basin is defined as a lower area or depression on the earth's crust that occurred due to the tectonic activity in which accommodation space is created for the preservation of sediments. They range in size from 100 meters to large ocean basins. Preservation of organic matter in a sedimentary basin in anoxic conditions leads to further hydrocarbon generation and further migration into sedimentary reservoir rock. In Pakistan, there are two main sedimentary basins in geological terms and genesis, including Indus Basin and Baluchistan Basin. Pishin Basin is a younger newly identified sedimentary basin of Pakistan also known as Kakar Khurasan Basin (Bender & Raza,1995).

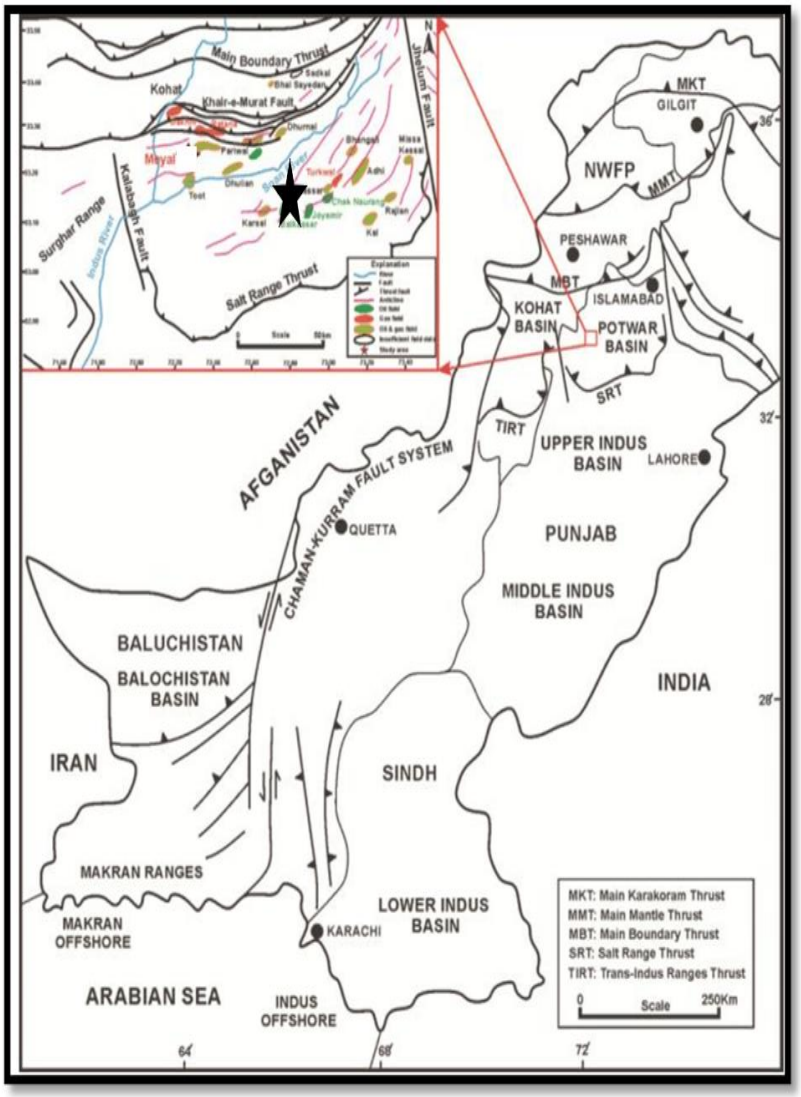

Figure 2.2. Map showing sedimentary basins of Pakistan (Aziz and Khan, 2003).

Upper Indus basin

Upper Indus Basin is situated in northern Pakistan and Sargodha highs separate it from the Lower Indus Basin. The main boundary thrust MBT bound the basin on its north and east side. The western boundary of the basin is marked by the uplift of pre-Eocene sediments and eastward directed thrusting to the Bannu (Kadri,1995).

The Upper Indus basin is further sub divided into two basins the Kohat sub basin and the Potwarsub basin. The Potwar sub basin is bounded by the river Indus from the west. There are two main unconformities marked in upper Indus basin between Permian and Cambrian time. In Potwar sub basin the important facies variation is the key character of this sub-basin. (Abid et al., 2019)

The study area is in the Eastern Potwar plateau of Upper Indus Basin which is in the northern part of Pakistan. Structurally the Soan syncline divides the Potwar sub basin into two zones, the Southern Potwar Platform Zone (SPPZ) which is less deformed and the Northern Potwar Deformed Zone (NPDZ). The study area is located below the Soan syncline in SPPZ (Abid et al. 2019).

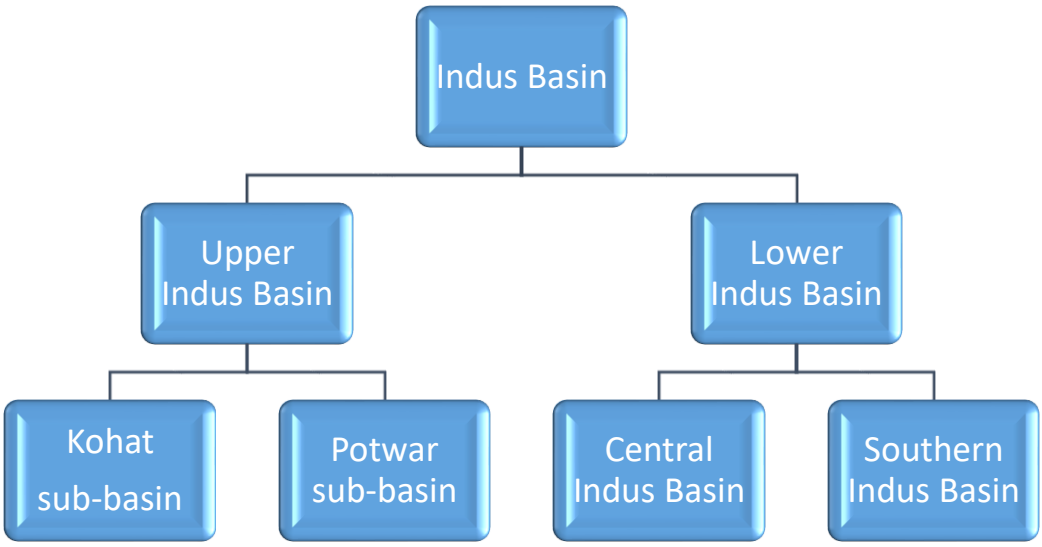

Figure 2.3. Divisions of Indus Basin.

2.3.1 Kohat sub-basin

West of Potwar sub-basin, lies the Kohat sub-basin in which Eocene sediments through Siwaliks are involved in a complex fold and thrust belt. This complex fold and thrust belt are characterized by Eocene salt which is occupied in many anticline's cores (Khan et al., 1986).

2.3.2 Potwar sub-basin

Potwar sub-basin is said to be the pioneer oil producing basin of Pakistan. It lies in the northern most edge of the Upper Indus Basin (Siddiqui and Aamir, 2006). The study area also lies in this basin. Potwar sub-basin is bounded by river Indus to the west and towards east it is bounded by river Jhelum in the zone of highly deformed and imbricate thrust sheet known as the Northern Potwar Deformed Zone (Lillie et al., 1987).

The sediments preserved in the Potwar sub-basin range from Pre-Cambrian to Quaternary age present in the subsurface and all of these are exposed in Salt range, southern most thrust. In the south of Kohat sub-basin lies the Trans-Indus ranges exposing sediments from Cambrian to Pliocene age. Both the sub-basins Potwar and Kohat are marked by an unconformity between Cambrian and Permian. Around the rim of the basin the sediments exposed are of Mesozoic age. However, the presence of these sediments is governed by Pre-Paleocene erosion which increasingly cut into older sequence from the Trans-Indus ranges in the west to east in Potwar basin through the Salt range (Khan et al., 1986).

2.4 Generalized stratigraphy

In Potwar sub-basin, the range of age of the sedimentary rocks is from pre-Cambrian to recent deposits. The major unconformities in Potwar sub-basin are from Ordovician to carboniferous, late Permian to Mesozoic and Oligocene. Salt range is made up of clastic deposits in lower section, carbonate deposits in middle section while halite deposits in upper section in which the potential source bed is recognized.

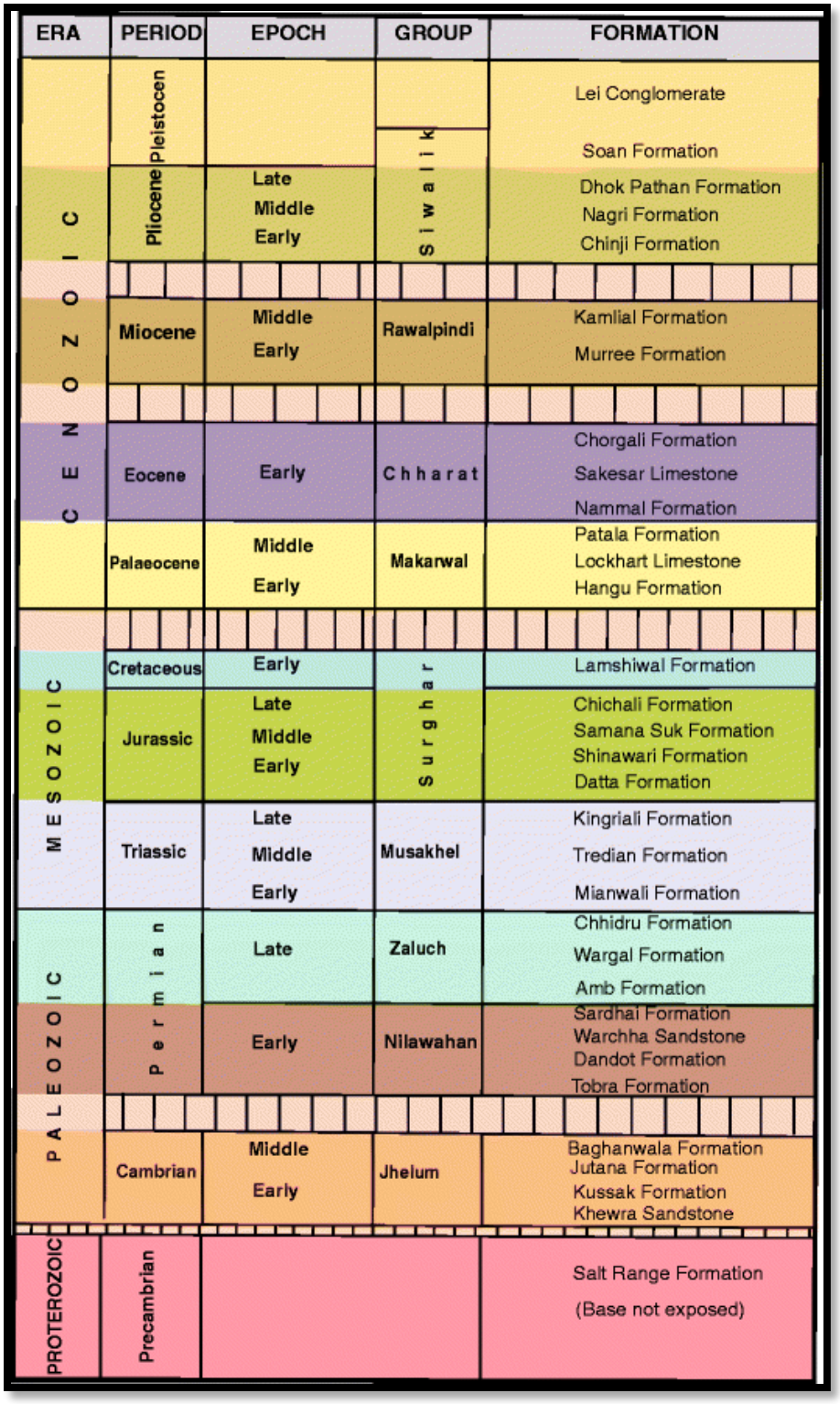

Figure 2.4. The generalized stratigraphic column of Potwar Basin (Ghazi et al., 2015)

2.5 Borehole stratigraphy

The well for study area is Balkassar Oxy-01. The stratigraphy is provided by LMKR and is given in the table 2.1. The total depth drilled in Balkassar Oxy-01 10266.5. The main reservoir in the study area is in Chorgali Formation and Sakessar Limestone.

Table 2.1. Borehole stratigraphy of well Balkassar Oxy-01 (provided by LMKR).

Age	**Formation Name**	**Formation Top (ft)**	**Thickness (m)**
Pliocene	Nagri Formation	0	1570.92
Pliocene	Chinji Formation	1570.92	3048.85
Miocene	Kamlial Formation	4619.77	349.98
Miocene	Murree Formation	4969.75	2974.85
Eocene	Chorgali Formation	7944.61	149.99
Eocene	Sakesar	8094.60	444.97
Paleocene	Patala Formation	8539.58	69.99
Paleocene	Lockhart	8609.58	114.99
Paleocene	Hangu	8724.57	89.99
Early Permian	Sardai	8814.57	359.98

Early Permian	Warcha	9174.55	464.97
Early Permian	Dandot	9639.53	199.99
Early Permian	Tobra	9839.521	169.99
Cambrian	Khewra Sandstone	10009.51	256.98
Pre-Cambrian	Salt Range Formation	10266.5	

2.6 Petroleum play

Petroleum system is basically a system comprising of all the important elements and processes that are essential for hydrocarbons to exist. The elements include source rock, reservoir rock, seal rocks and traps. The processes include generation, migration, accumulation, and preservation of hydrocarbons (Ishimwe, 2014).

2.6.1 Source rock

Patala Formation of Paleocene age are a potential source rock in the study area (Khan et al., 1986). the oil shales of Eo-Cambrian Salt Range Formation have 27-36% TOC. There are small pockets of shale which are considered as a source rock in SRPFD (Shami and Baig, 2003).

2.6.2 Maturation

Maturation is a principal quality indicator of hydrocarbons present in the reservoir. The values of thermal maturation for Kohat-Potwar rocks are in the range of Ro 0.3-1.6% (Jadoon et al.,1999).

2.6.3 Generation and migration

The migration and generation of hydrocarbons is believed to be started in the late Cretaceous. The migration for Cambrian source rock occurred through Late Cretaceous from Pliocene to recent times for the younger source rocks (Jaswal et al., 1997).

2.6.4 Reservoir rocks

The reservoir of Cambrian, Permian, Jurassic, Paleocene, and Eocene are producing oil in salt in SRPFD. The highly fractured carbonates of Sakessar Limestone and Chorgali Formation are major producing reservoir rock in Balkasar area (Hasany and Saleem, 2001).

2.6.4 Cap rock

Rawalpindi group of Miocene age act as a cap rock for the reservoirs of Chorgali Formation and Sakessar Limestone of the Eocene age. The shales and clay of Murree Formation provide efficient seal over vertical and lateral directions to Eocene reservoir in SRPFD.

CHAPTER 3

SEISMIC INTERPRETATION

3.1 Introduction

Seismic interpretation is the method in which we delineate the subsurface structural and stratigraphic image with the help of seismic data that is obtained by seismic acquisition. With the help of velocities and the time data we mark the horizon and convert the velocity data into depth by the inversion method. The focus of seismic data interpretation is to map the subsurface to get the knowledge of the subsurface using seismic data. Recording principle of seismic data is based on arrival times of reflections and rare fractions from the subsurface (Yilmaz, 2001).

The principle of acquisition is that we have a source that generates the seismic wave at a particular array position and specific frequencies of these waves along with its shape move to subsurface and then strike back to the surface which are then recorded on the specific geophones installed in the array. The geophone converts the mechanical energy into electrical signals that are shown as a wiggle and the specific shape of these wiggles known as phase. through phase delineation and amplitude variation we identify the fluid content and the lithology of subsurface (Dobrin and Savrit,1988). There are two main categories of interpretation:

1. Structural interpretation
2. Stratigraphic interpretation

3.1.1 Structural interpretation

The main objective of structural analysis is to locate structural trap. Structural traps include inferring about the geometry of reflector. It helps to analyze the geological structures like synclines, anticlines, faults etc. to determine the reserves of hydrocarbons. So, structural interpretation plays an important role in understanding the tectonic behavior of study area (Yilmaz, 2001).

There are two main tectonic regimes that develop these tectonic structures which are the compressional and extensional regimes respectively. In compressional we have

geological structures like diplex structures, synclines and recumbent folds, anticlines, and popup structures and reverse and thrust faults. In extensional regimes the geologic structures like horst and grabens, normal faulting in which the hanging wall moves down to the footwall are obtained. In our study area we observe the thrust fault, a large anticline popup structure.

3.1.2 Stratigraphic interpretation

Stratigraphic interpretation is the based upon reflection patterns and these patterns when are associated with the model, they represent the cyclic deposition of the strata that genetically relate to each other. A stratal surface is a deposition of bending plane, marine flooding surfaces which define a fix geologic time. In case of siliciclastic rocks, that deposit in a high accommodation environment containing numerous vertically stacked stratal surfaces.

There are two dimensional layers that represent the stacking patterns of different para-sequential geometries deposit at time or the change in relative sea level. In oceanic basin the hydrocarbons are mostly associated with the stratigraphic traps that are formed by down lap or onlap geometry. These geometries are basically the stratigraphic traps that trap the hydrocarbon and act as a direct hydrocarbon indicator (DHI). There are different types of stratal surfaces, flooding surfaces, erosional surfaces, maximum flooding surfaces. In the stratigraphic interpretation the key step is interpretation of these stratigraphic traps using well logs, core, and seismic data. Stratigraphic interpretation is more complex than structural interpretation (Joncheray et al.,1978.).

3.2 Seismic interpretation workflow

The workflow for seismic interpretation is shown in methodology section of chapter 1 (Fig 1.3).

3.3 Methodology

The methodology of seismic interpretation involves the following steps:

3.3.1 Base map generation

The generation of base map is done using the software Kingdom 8.8 with the help of navigation files obtained from LMKR. 3 strike and 3 dip lines were obtained which gave information about shot points, well location. We created the well location through well log coordinates given on log header and the software generated the well point which gave us our control line. We generated the base map on the scale of 1:378647.

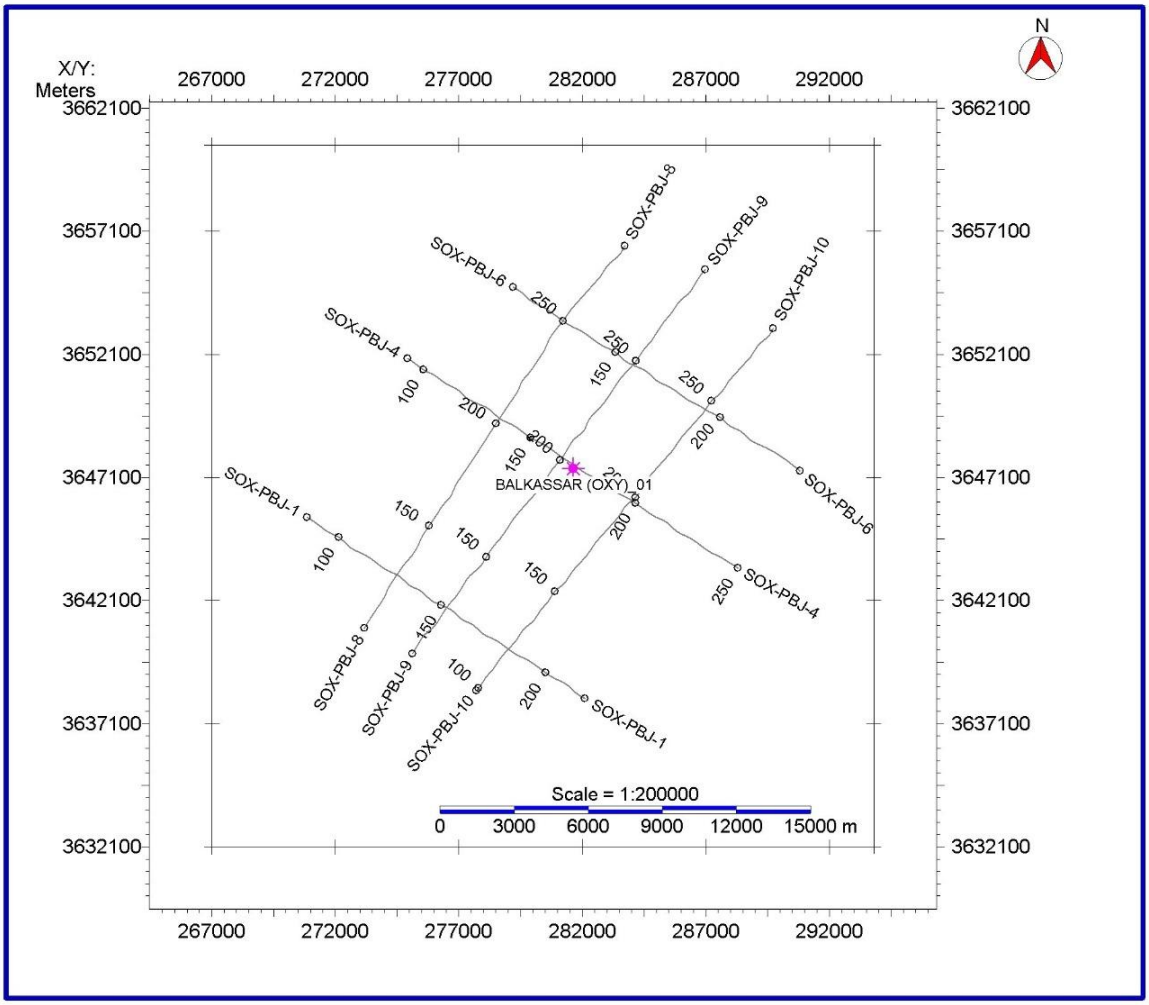

Figure 3.1. Base map of study area.

3.3.2 Selection of control line

It is the seismic line upon which the well is located after the generation of base map, we select the control line. In our study area, Balkassar Oxy-01, the well is located on

the seismic line SOX PBJ-04. The well is located near the shot point 173 of the seismic control line. After the selection of control line, we perform the well to seismic tie.

The depth of the horizons was correlated with seismic data depth with the help of both seismic and log data which are acquired with different reference datum. The correlation of both depths is done by equating well datum (KB) and seismic datum (reference datum). We use a mathematical equation that is derived by Francis in 2018.

$$FD=FT+KB-SRD \qquad (3.1)$$

Here, FD= Formation depth, FT=Formation Top, KB=Kelly Bushing, SRD=Seismic reference datum.

We use this equation to calculate formation depth, the value of known variables for example, formation top that is given in the well tops data, the value of KB and SRD is taken from well header and seismic section respectively. By putting the values of formation top, KB and SRD we calculate the formation depth for our targeted formations i.e., Chorgali Formation and Sakessar Limestone. When the depths are calculated then by using the seismic window given in the seismic section, we plot these data values on excel sheet and generate Time-Depth Chart. The use of TD chart is to mark the values of time for extending the horizons on the seismic section.

Table 3.1 Calculation of formation depths.

Formation Name	**FD=FT+KB-SRD**	**Formation Depth (m)**	**TWT(s)**
Chorgali Formation	2479.518+350-535	2293.518	1.24s
Sakessar Limestone	2528.236+350-535	2342.236	1.25s

3.3.3 TD chart of Balkassar Oxy-01 well

After the selection of control-line we generate a TD chart (Time-Depth chart) using velocity, time, and depth data. These data sets were obtained from the seismic section that is given in a seismic window and these values are put on the excel sheet which in turn is used to generate a graph of time and depth respectively. According to depth we mark a

time value on the TD chart which is further used for extension of horizon lines. The time given on the seismic section is two-way travel time i.e., when waves hit an interface boundary and return to the geophones. But for depth we only need one way travel time i.e., when the wave is returning to the surface after hitting the boundary thus, we divide the TWT by 2000 which covers the seismic TWT to one way domain. The depth is calculated by using Sigismund (2018).

$$S=V*t/2000 \qquad (3.2)$$

Here, S= depth, V= velocity and t= time.

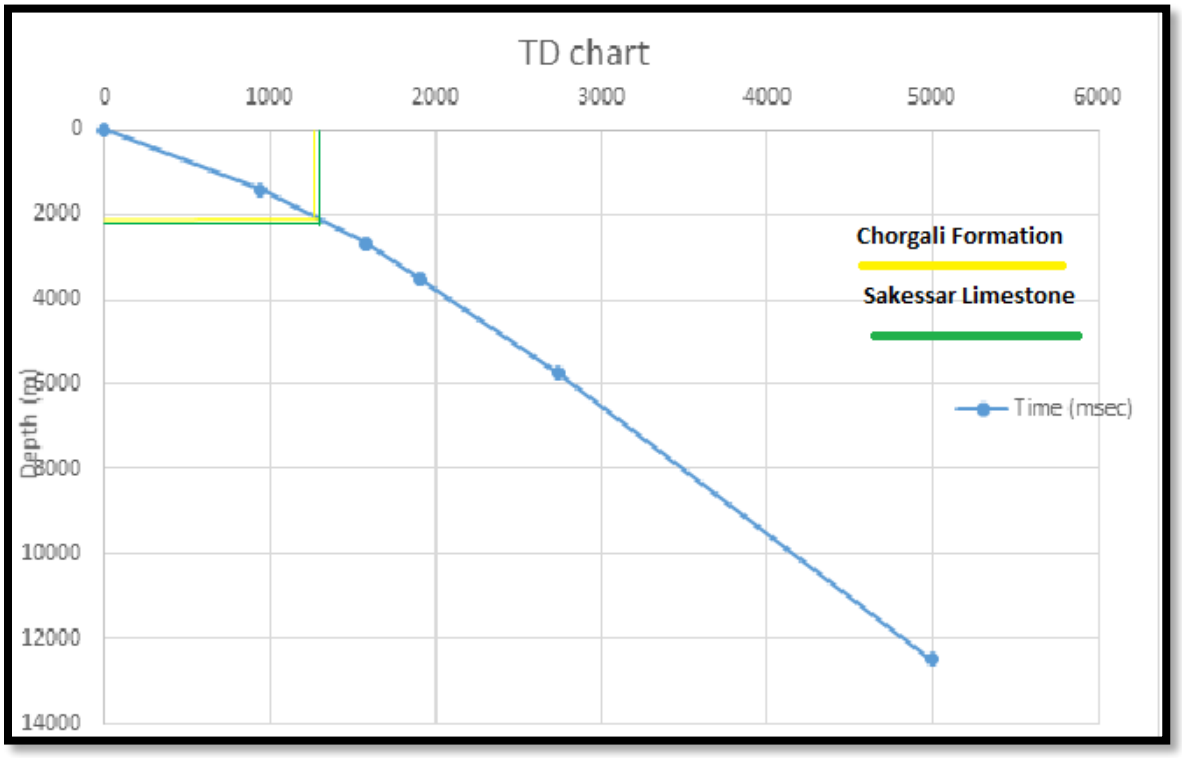

Figure 3.2 Time depth chart.

3.3.4 Horizon marking

After the generation of T-D chart we would mark the horizons on the seismic section. The time obtained from the TD chart that is 0.75 and 0.8 for Chorgali Formation and Sakessar Limestone respectively. Then we mark the horizon on the three strike and three dip lines and will extend the line with respect to our time that is obtained on the TD

chart. Our control line is SOX PBJ-04 in which we mark the horizon from shot point 130-250 which are common shot points for all seismic lines.

3.3.5 Fault identification and marking

After marking the horizon on the seismic section, we mark the fault according to the displacement of strata that is shown in the section in the form of reflector displacement. In our study area we mark a popup structure, broad anticline, on the seismic line SOX PBJ-04 which is our control line. This popup structure represents the geological location of our study area which is a compressional tectonic regime.

3.3.6 Interpretation of seismic lines

We have three dip lines and three dip lines which are SOX PBJ-01, SOX PBJ-04, SOX PBJ-06 which are the dip lines and SOX PBJ-08, SOX PBJ-09 and SOX PBJ-10 are the strike lines. This data is provided by the LMKR department which has a very low resolution and a low quality which is maximum 40-fold data at each seismic line. The seismic section of the study area represents the geological structures like anticlines and popup geometry.

According to these geometric structures, our study area lies in a compressional tectonic regime. We mark the two reflector, Chorgali Formation and Sakessar Limestone on a dip line SOX PBJ-(04, 01, 06) along with the strike lines SOX PBJ-(08, 09, 10). Interpreted seismic section is shown below.

The well lies in the shot point 173 of control line SOX PBJ-04. This dip line is perpendicular to major structure which is a popup geometry and considered as more suitable for geologic interpretation. The dipping direction of fault is NW-SE and lies at line SOX PBJ-04 shot point from 135-205 with interval of 5. We tie this dip line (SOX PBJ-04) with SOX PBJ-08 at shot point 202, line-09 at shot point 203 and line 10 at shot point 200. SOX PBJ-(08, 09, 10) show F4, F5, F6 Which are not controlling the major structure, but overall, it shows the extent of anticline structure that is present on the dip line SOX PBJ-04. Below mentioned figure 3.3 is the interpreted seismic line SOX PBJ-04 which shows a broad anticline structure.

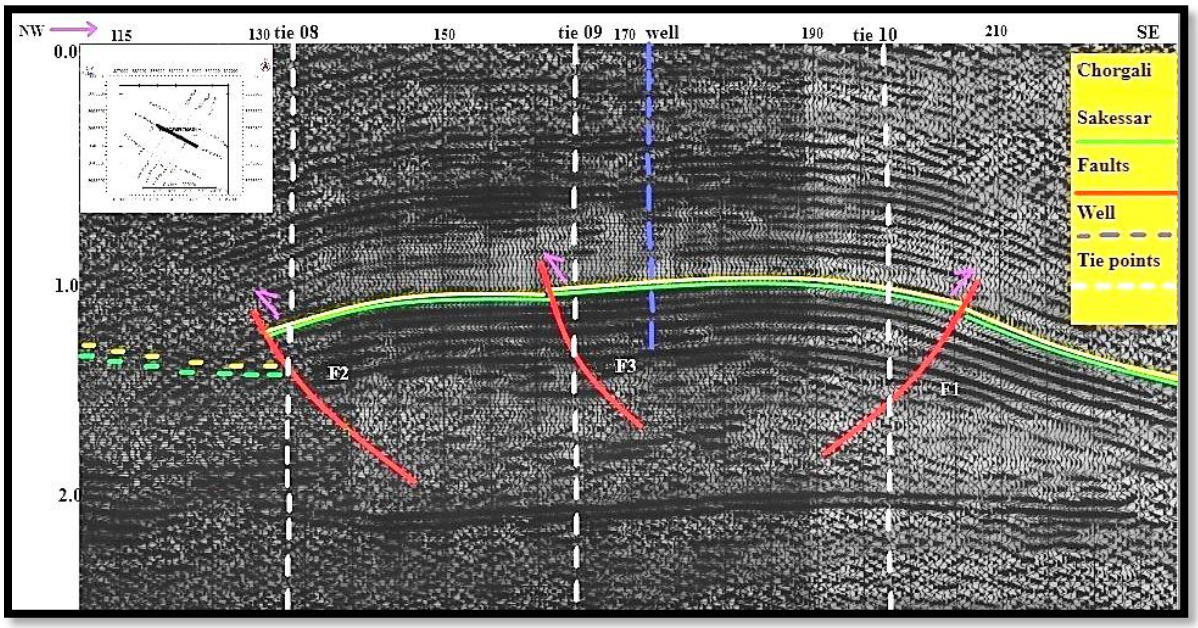

Figure 3.3 Interpreted control line SOX PBJ-04.

The next dip line is SOX-PBJ 01. The dip line shows the orientation of structure and its shape. It is orientated in the NW to SE directing holding shot points from 100 to 200. This dip line seismic section shows the anticline, Popup Geometry structure present on SOX-PBJ 04. It has Three Faults F1, F2, F3 which are major fault that control structure present on seismic line SOX-PBJ-04. This lies ties with strike lines SOX PBJ 08 at S.P 127. The seismic section is shown in figure 3.4:

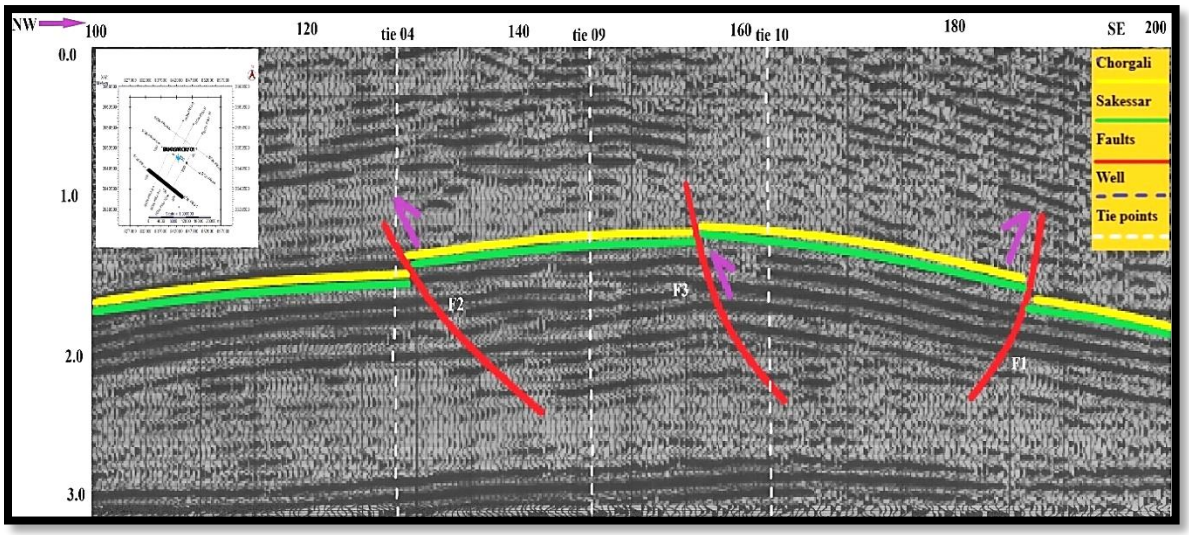

Figure 3.4. Interpreted SOX PBJ-01.

Next dip line namely SOX-PBJ 06. This dip line seismic section shows a complete pop-up structure having three faults which are located on S.P 140, 170 and 205

respectively. This section holds shot points from 120 to 220. The orientation of this dip line is also NW to SE. Being a dip line, this line runs perpendicular to the major pop-up structure.

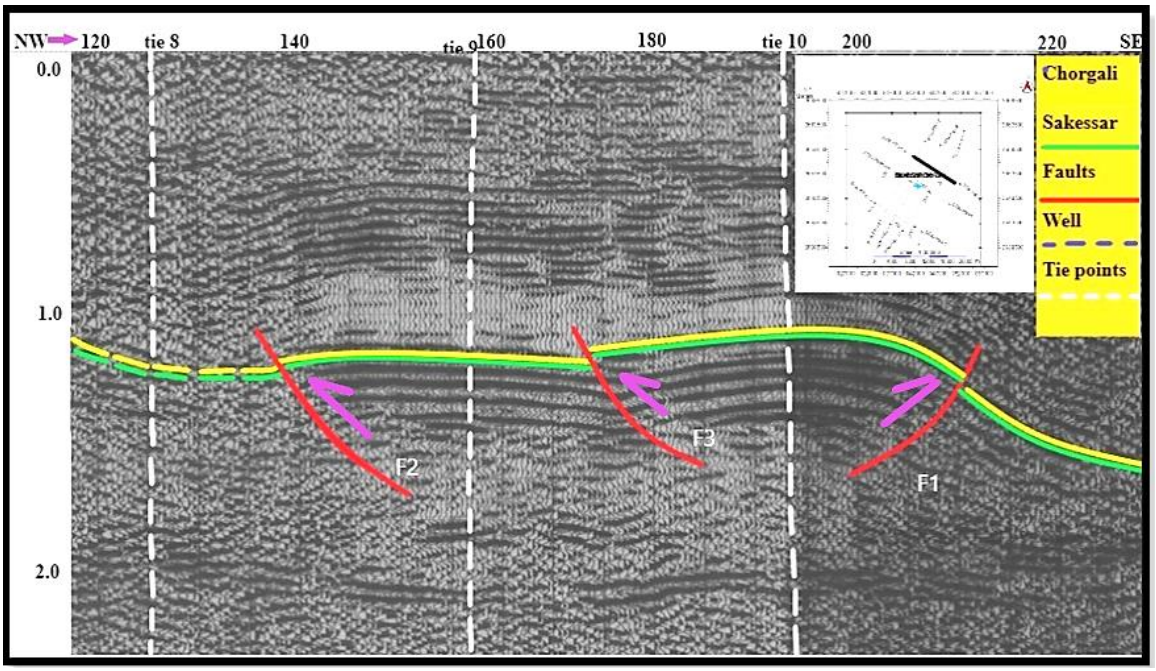

Figure 3.5. Interpreted seismic line SOX-PBJ 06.

F1 is a northwest dipping thrust fault and F2 is a SE dipping thrust fault. The F1 is a major thrust while F2 is a back thrust fault.

The next seismic line is SOX-PBJ 08 which is a strike line in the direction SW to NE holding shot points from 130 to 270. The seismic section of this line shows a F4 Fault which dip NW direction. The overall seismic section shows the extension of anticline structure present on PBJ-04. We mark the Chorgali Formation and Sakessar Limestone at the TWT 1.24 and 1.25 respectively.

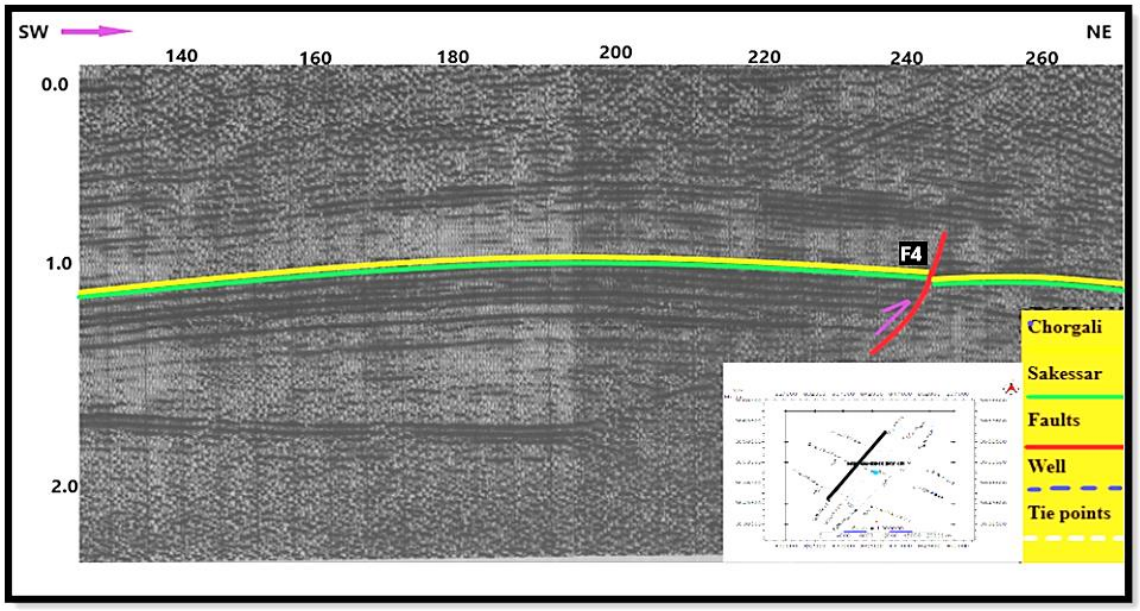

Figure 3.6. Interpreted seismic line SOX-PBJ 08.

The strike line SOX-PBJ 09 orienting in the NE-SW direction holding shot points from 125-275. This line shows an F5 fault at shot point 145 dipping in the SE direction. Overall this line shows the exension of the anticline structure present on SOX-PBJ 04.

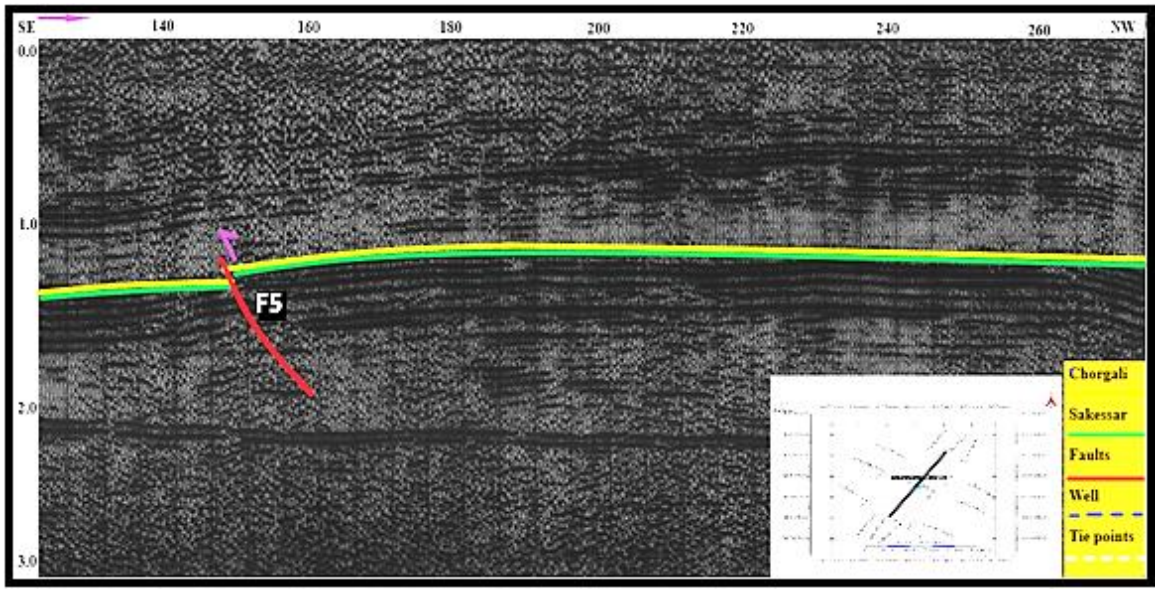

Fig 3.7 Interpreted seismic Strike line SOX-PBJ 09

The strike line SOX-PBJ 10 oriented in the SE-NW direction, holding shot point from 120-270. Marked fault F6 is shown at shot point 138 but overall structure represents the extension of the anticline shown on the seismic line SOX-PBJ 04.

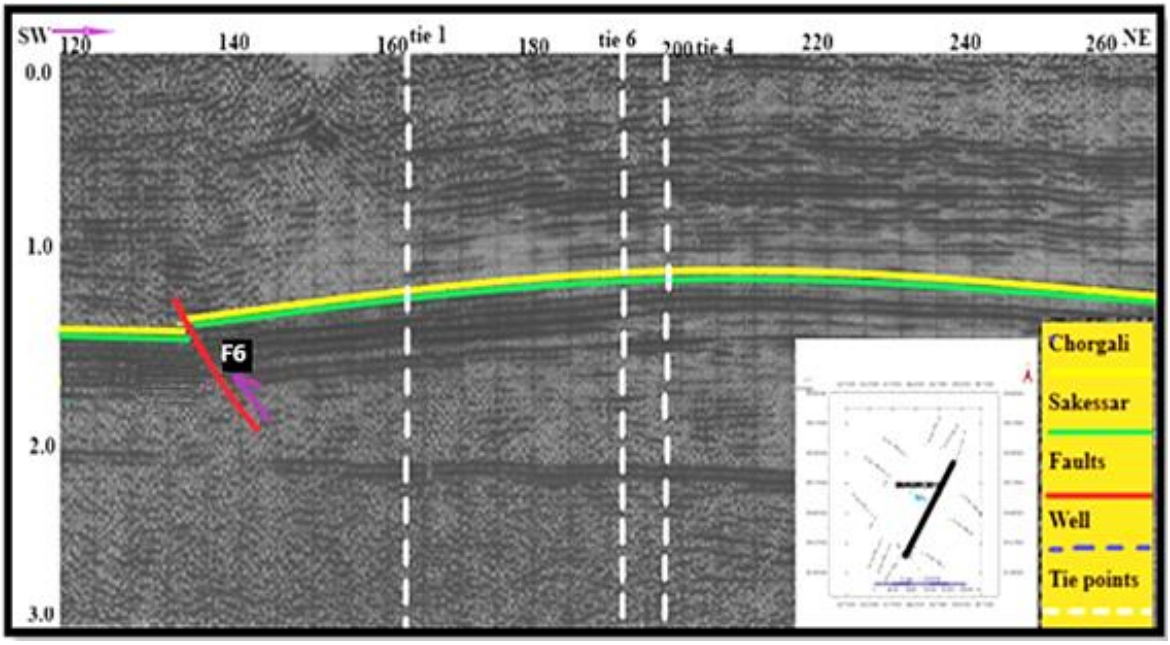

Figure 3.8. Interpreted seismic line SOX-PBJ 10.

3.3.7 Time picking

It is a very important method for the generation of time-contour map. Without time picking time-contour map cannot be generated because the time contour map shows the justification of the structures present on the seismic section. The time values of Chorgali Formation and Sakessar Limestone are picked with the help of the time scale present on the sides of the seismic section. All of the seismic lines have a shot point interval of 5. While picking time, when we move from one seismic line to another, we take in consideration the exact value of time at the intersection of the strike and dip lines for all of the six seismic lines.

3.3.8 Contour maps

The generation of contour maps is done after time picking. It defines the justification of structure on the seismic section present in the sub surface. It is a very repititive process. The 2D input data is used in the form of x,y (Latitudes and Longitudes) and Z (time). All of these values are put in the the Kingdom 8.8 software which generates a contour map for us. With the help of these contour maps we dilineate the folding, faulting,dipping and slope of the subsurface structures.

3.3.8.1 TWT contour maps

The Twt contour shows the same time value at every contour line. The TWT i.e. wave hitting an interface boundary and returning back to geophones is recorded. The time contour maps for both Chorgali Formation and Sakessar Limestone at every 5 shot point interval and the same is done for dilineating the faults. Contour map shows the exact location of the pop-up, anticline structure that is present at the study area.

For Chorgali Formation, we pick the time at the top of Chorgali Formation with contour inerval set as 0.05 s that shows the different color variation. Light color shows less time and shallower depth and Dark colors show larger time values with deeper depths respectively. The faults F1 and F2 are shown with help of these contour maps. Both these faults enclose the pop-up structure with F1 as a major thrust dipping in the SE direction and F2 as a backthrust dipping in the NW direction. A broad anticline structure shown in the contour maps justifies the contour time and its red color. The contour passes from well location that time has 1.24s

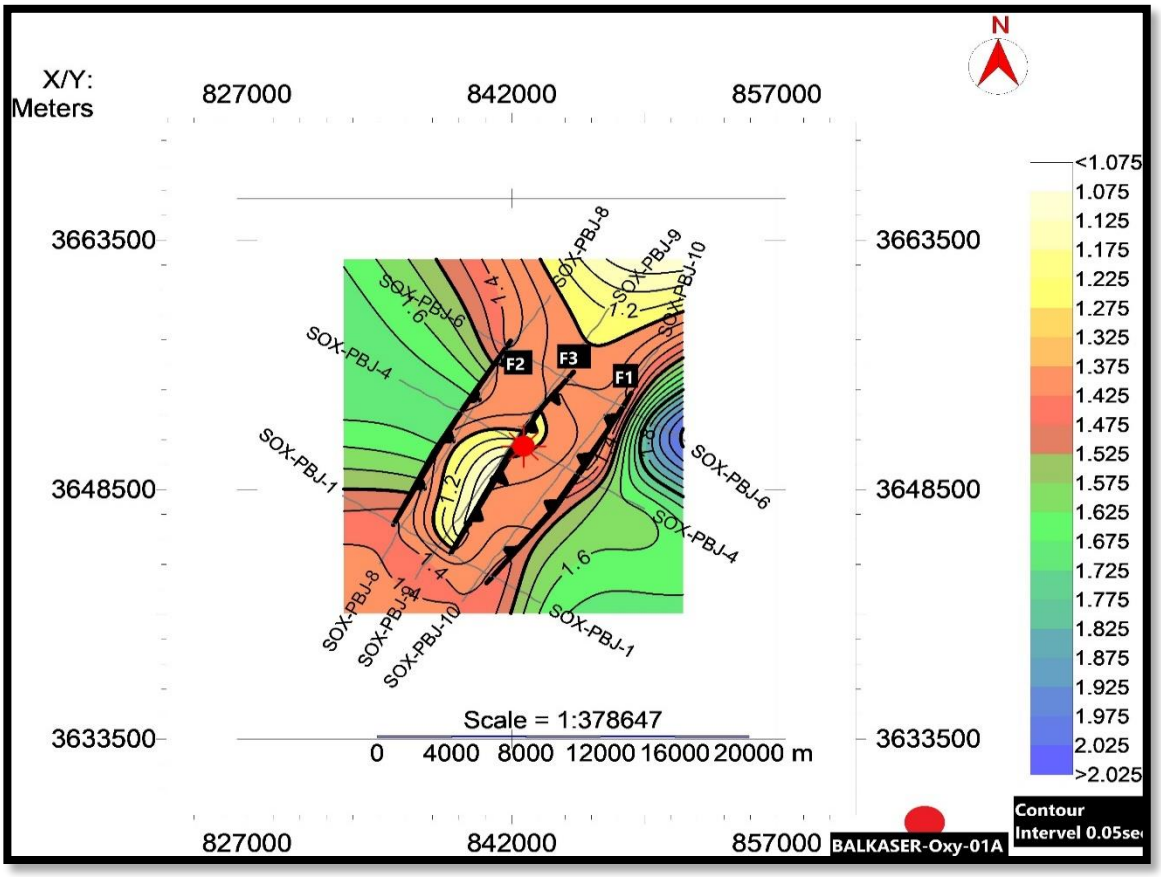

Figure 3.9. Time contour map Chorgali Formation.

The next formation is Sakessar Limestone that is shown in fig 3.10. The time contour map of Sakessar Limestone shows a pop-up strucutre bounded by F1 and F2 thrust faults. The horizon of this formation shows a shallower depth values at lesser time. The contour interval for this formation is 0.050s and the contour lines which pass through the well give a time value of 1.25s

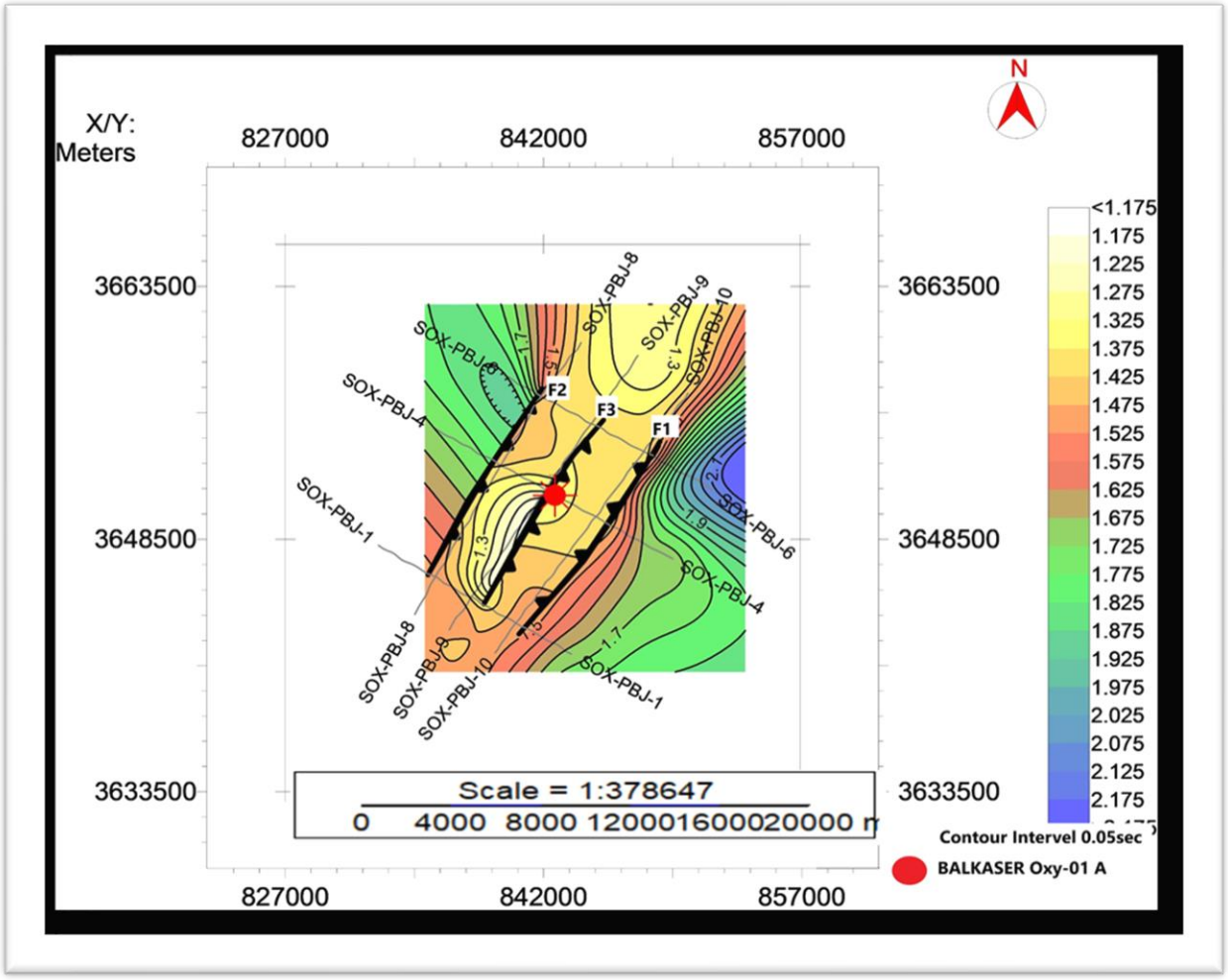

Figure 3.10. Time contour map of Sakessar Limestone.

3.3.8.2 Velocity calculation

Our next step is generation of depth contour maps which require velocity values given on the seismic lines in the form of seismic windows that have three columns of time, velocity, and instantaneous velocity. We pick the time against its velocity value and these values are put in Excel sheet and the gap between these values is filled a function of MS

Excel which is called “Series fill”. Next, we use the time value against each formation and convert the TWT into milliseconds because in the seismic window the time is given in milliseconds. For selection of velocity value against time, it should be in the milliseconds. After picking velocities we put it in the Sigismund (2018).

$$S=V*t/2000 \qquad (3.3)$$

3.3.8.3 Depth contour maps

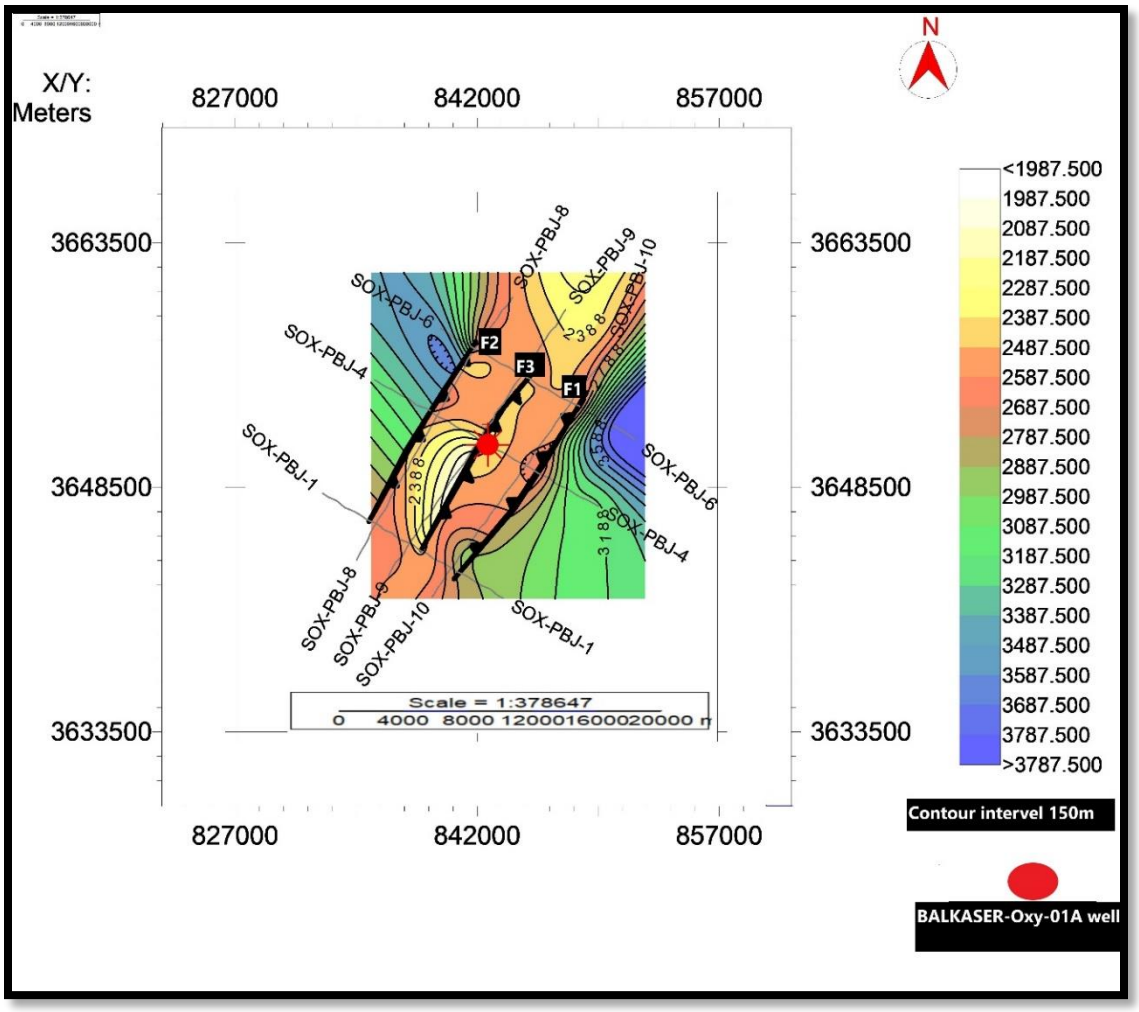

Figure 3.11. Depth contour map of Chorgali Formation.

The depth contour map shows the values of same depth at each intersection point of seismic lines. Depth maps are used for calculating the structure depth and later for the total target depth for drilling. Light colors show shallow depth and dark colors show deeper

depths. In our study area, the pop-up structure has a shallower depth value. The contour line passing through the well has a depth value of 2293m. In this formation the depth contour interval was 150m.

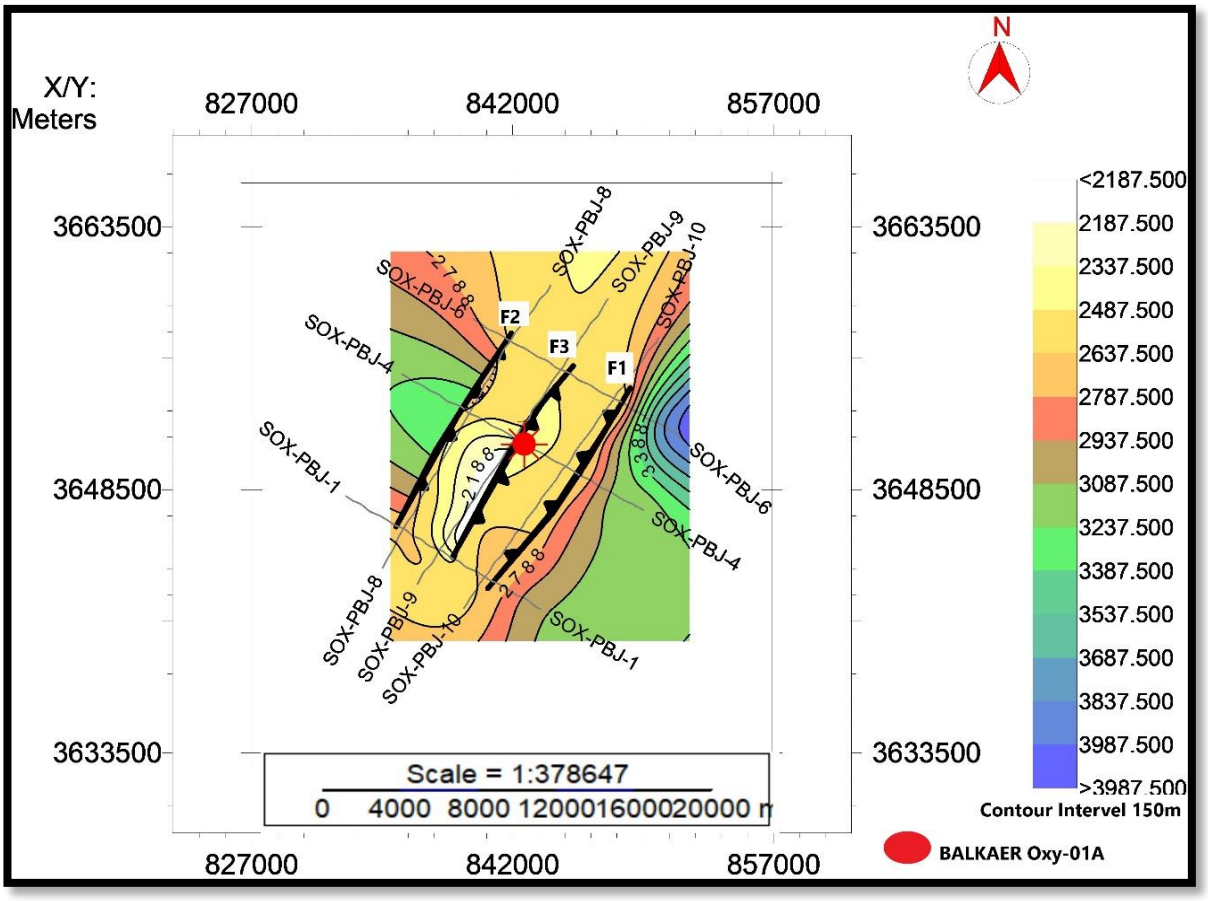

Figure 3.12. Depth contour map of Sakessar Limestone.

The depth map of Sakessar Limestone is shown in the figure 3.12 . It also shows a shallow depth horizon with lighter color and the contour line passing through the well gives a depth value of 2342m. The contour interval is set at 150m.

CHAPTER 4

PETROPHYSICAL ANALYSIS

4.1 Introduction

Petrophysical analysis is defined as the analysis of formations through well log data which is acquired by drilling. Petrophysical analysis is the key method for marking the potential hydrocarbon zone (Ellis, 1987). The petrophysical parameters like porosity, depth, temperature, Grain size, Volume shale and volume of clean (Rider, 1996, Sarastay and Stewart 2003) pressure and the reservoir characterization is based on these parameters are directly related with the production of hydrocarbon (Joshi et.al 2004). The petrophysical analysis is done for discrimination of reservoir zone and economic volubility of the proven reserves present in the area. The petrophysical analysis is a wide range intra disciplinary study that is directly to exploration geophysics, petroleum engineering and geology.

2.2 Workflow of petrophysical analysis

The workflow for petrophysical analysis is shown in methodology section of chapter 1 (Fig 1.4).

4.3 Marking the zone of the interest

The zone of interest zone is defined as a probable hydrocarbon containing zone with acts as a prospect. We mark the zone of interest with the help of leg trends. When the gamma ray log values fall on the lower side it forms a cleaning upward trend which indicate the coarsening of lithology. In contrast, when the gamma ray values fall on the higher side, it forms the dirtying upwards trend indicating the fining of particles in the lithology. The Caliper log should be stable, and the value of caliper log should be <= bit size. The resistive log is very sensitive towards fluid and the place where resistivity log values are high, we indicate a hydrocarbon bearing zone and the order of resistivity log should be, MSFL<LLS<LLD.

The Bulk Density and Neutron Porosity log which show a crossover relationship in which the values of Density and Porosity log move toward the lower scale. The self-potential log shows a negative deflection.

4.4 Well Statistics

The well statistics were provided by LMKR with the log data. These statistics are shown in table 4.1.

Table 4.1. Statistics of Balkassar Oxy-01 well.

Well Name	Balkassar Oxy-01
Well Type	Exploratory
Well Status	Abandoned
Operator	OXY
Run date	28th August 1981
Lat/long	32˚06'38.8" N /72˚ 39'52.5" E
Province	Punjab
Concession	Chakwal
Total depth	8710ft
Depth Reference	KB
Depth Ref. elevation	535.53m
Formation Top	Chorgali Formation 2421.518m, Sakessar Limestone 2467.213m
Well Bore name	Oxy-Balkassar#1
Well Bore status	Abandoned

4.5 Formation Evaluation

The Chorgali Formation was evaluated on the criteria mentioned in the section 4.3. Chorgali Formation starts at 7943 ft and ends at 8094 ft. Only from the depths of 8020ft to 7050ft we mark our ZOI because all the criteria mentioned in the above heading are fulfilled in this zone. In case of Sakessar Limestone we mark the whole formation, which starts from 8100ft to 8540ft. We evaluate the logs data at every 5ft depth and calculate the different petrophysical parameters. Formation evaluation is given the table 4.2.

In Chorgali Formation, the zone of interest shows that the gamma ray curves on the lower side and the caliper log is much stable in the zone of interest, and we can calculate the neutron porosity directly from the well data and for the Density porosity, we calculate the value of Rhob. There is a little separation between resistivity logs (MSFL and LLD) that is also a criterion for marking the zone of interest. But the SP log shows positive deflection.

For Sakessar Limestone, we did not calculate the density porosity and neutron porosity where the correction factor value was higher +-1.5 and the Sakessar Limestone has a total 6 number of depths where the caliper log is not stable, and the correction value factor is also greater than 1.5.

Table 4.2 characteristics of Chorgali Formation and Sakessar Limestone in Balkassar Oxy-01.

Formation evaluation for reservoir potential					
Formation name	Geological age	Lithology	Starting depth	Ending depth	Total thickness
Chorgali Formation	Late Eocene	Limestone	7943ft	8095ft	152ft
Sakessar Limestone	Late Eocene	Limestone	8095ft	8540ft	448ft

4.6 Logging while drilling details of Balkassar Oxy-01 well

The details of Balkassar Oxy-01 were provide by LMKR after approval from DGPC. The details are provided in the table 4.3.

Table 4.3. Logging and drilling details of Balkassar Oxy-01 well.

Logging interval	Top log Interval=7965ft Bottom log interval=8692ft
Drilling Fluid	Lignosulphonate
Maximum recorded temperature	180°F
Bit Size	8.5 inches
Formation considered for reservoir evaluation	Chorgali Formation and Sakessar Limestone

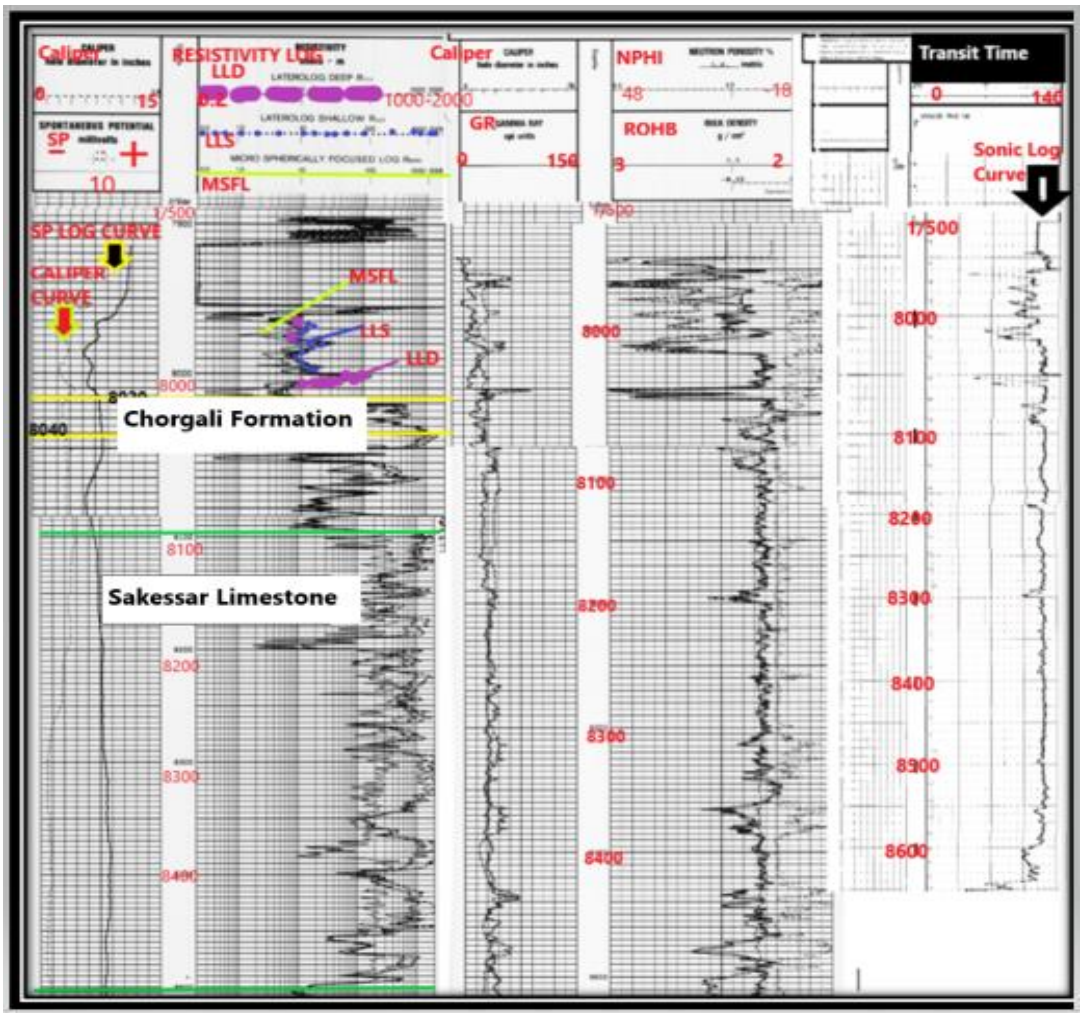

Figure 4.1. Potential reservoirs in Balkassar Oxy-01

4.6.1 Calculation of Vshale

Vshale indicates the amount of shale in a particular formation. Volume of shale calculated through Schlumberger equation (1972).

$$V_{sh} = I_{GR} * 100 \qquad (4.1)$$

$$I_{GR}=\frac{GR_{Log}-GR_{Min}}{GR_{Max}-GR_{Min}} \qquad (4.2)$$

Here, V_{SH}=Volume of shale, I_{GR}= Shale index, G_R Log= Gamma ray log values (unit, API), G_r minimum= minimum value gamma ray log (unit, API), Gr maximum= maximum value gamma ray log (unit, API).

4.6.2 Volume of clean

It represents how much a formation is clean or dirty which is calculated by using the following equation (Schlumberger, 1972)

$$V_{clean}=1-V_{shale} \qquad (4.3)$$

4.6.3 Porosity calculation

Porosity calculation is a key step for reservoir evaluation. In hydrocarbon bearing zones the effective porosity must be high because when pore spaces are properly connected, it allows better movement of hydrocarbon which is termed as permeability. The area with more proper connected spaces, there is high effective porosity. The following calculations are made to calculate the effective porosity from log data.

4.6.3.1 Neutron porosity

Neutron porosity is directly calculated from the neutron log at the depth of interest. Neutron log is the direct indicator of porosity.

4.6.3.2 Density Porosity

Density porosity is calculated from bulk density values at depth of interest via following formula (Tiab and Donaldson, 2004).

$$\Phi = \frac{(pma-pb)}{(pma-pf)} \qquad (4.4)$$

Here, Φ = density porosity of the rock, pma = Matrix density, pb = bulk density of the formation, pf = density of fluid.

4.6.3.3 Sonic porosity

Sonic porosity is calculated from sonic log using the value of (Δt)

$$\Phi s = \frac{\Delta t - \Delta t_{ma}}{\Delta t_f - \Delta t_{ma}} \qquad (4.4)$$

Here, Φs= sonic porosity of rock, Δt = transit time from log, Δt_{ma}= matrix time (taken as 47.6 for limestone), Δt_p = transit time of fluid (taken as 185).

4.6.3.4 Average porosity

It is calculated by adding density and neutron porosity and taking their average. Where the Density and neutron porosity is not reliable, we use the value of sonic porosity. The average of neutron porosity and density porosity is taken as average porosity (Tiab and Donaldson, 2004).

$$\Phi avg = \frac{(\Phi s + \Phi N)}{2} \qquad (4.5)$$

4.6.3.5 Effective porosity

Effective porosity is calculated by the formula

$$\Phi e = \Phi avg * (1-V_{sh}) \qquad (4.6)$$

Here, Φe = Effective porosity, Φavg = Average porosity, V_{sh} = Volume of shale

4.6.4 Resistivity of water (Rw)

To find the water saturation in rocks, firstly we must find resistivity of water that is calculated by the following steps (Dewan, J.T., 1983).

In step one, the geothermal gradient is calculated by using the following equation:

$$\text{Geothermal gradient} = \frac{\textbf{borehole temperature} - \textbf{surface temperature}}{\textbf{total depth}} \qquad (4.7)$$

Geothermal gradient=0.0105^{o}F

The next step is calculation of formation temperature using the following formula:

Formation temperature = (Formation top * geothermal gradient) + surface temperature (4.8)

The third step is calculating resistivity of mud filtrate (Rmf) at surface temperature which is then converted to Rmf at formation temperature using GEN-9 chart.

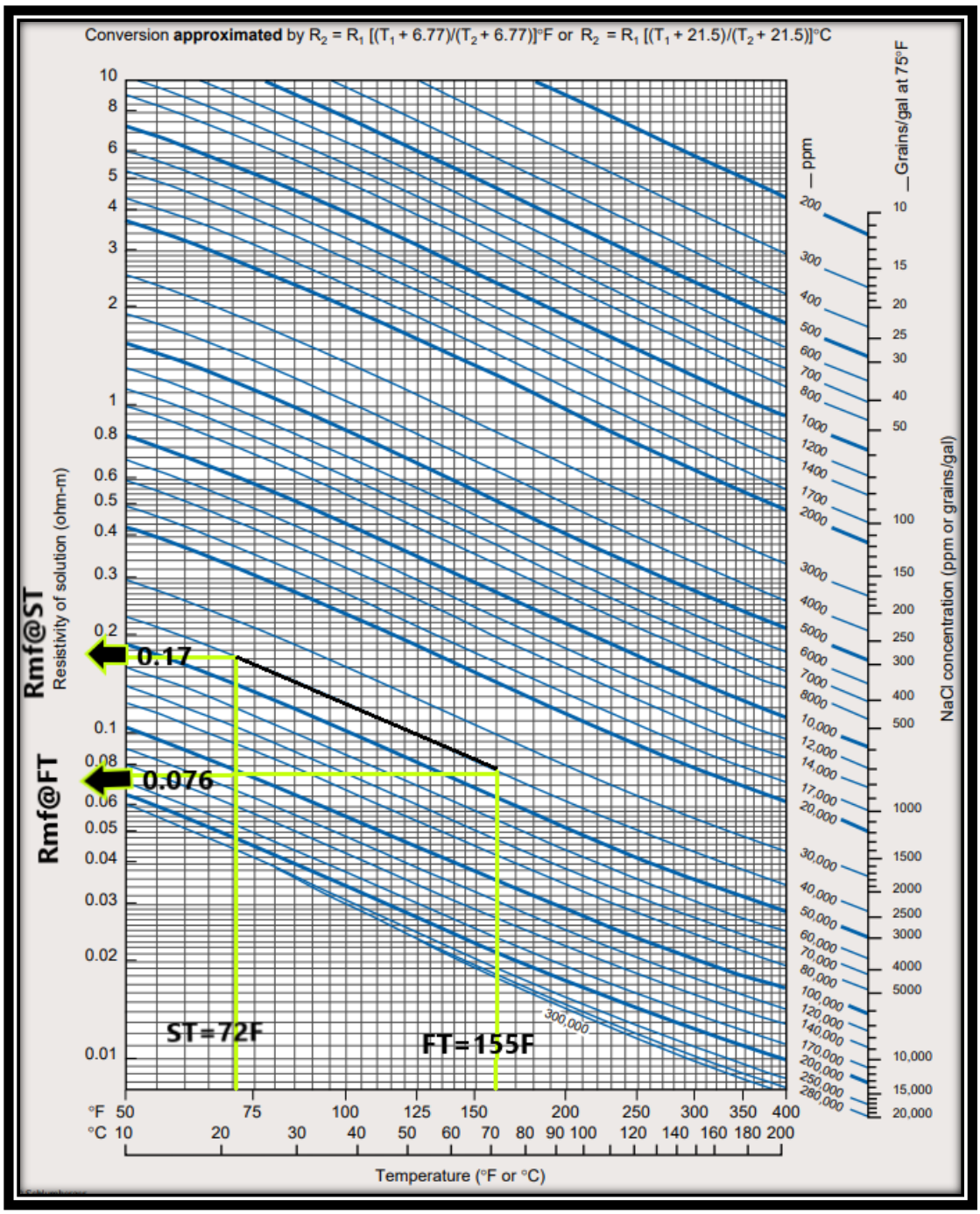

Figure 4.2. Gen-09 Chart of Chorgali Formation.

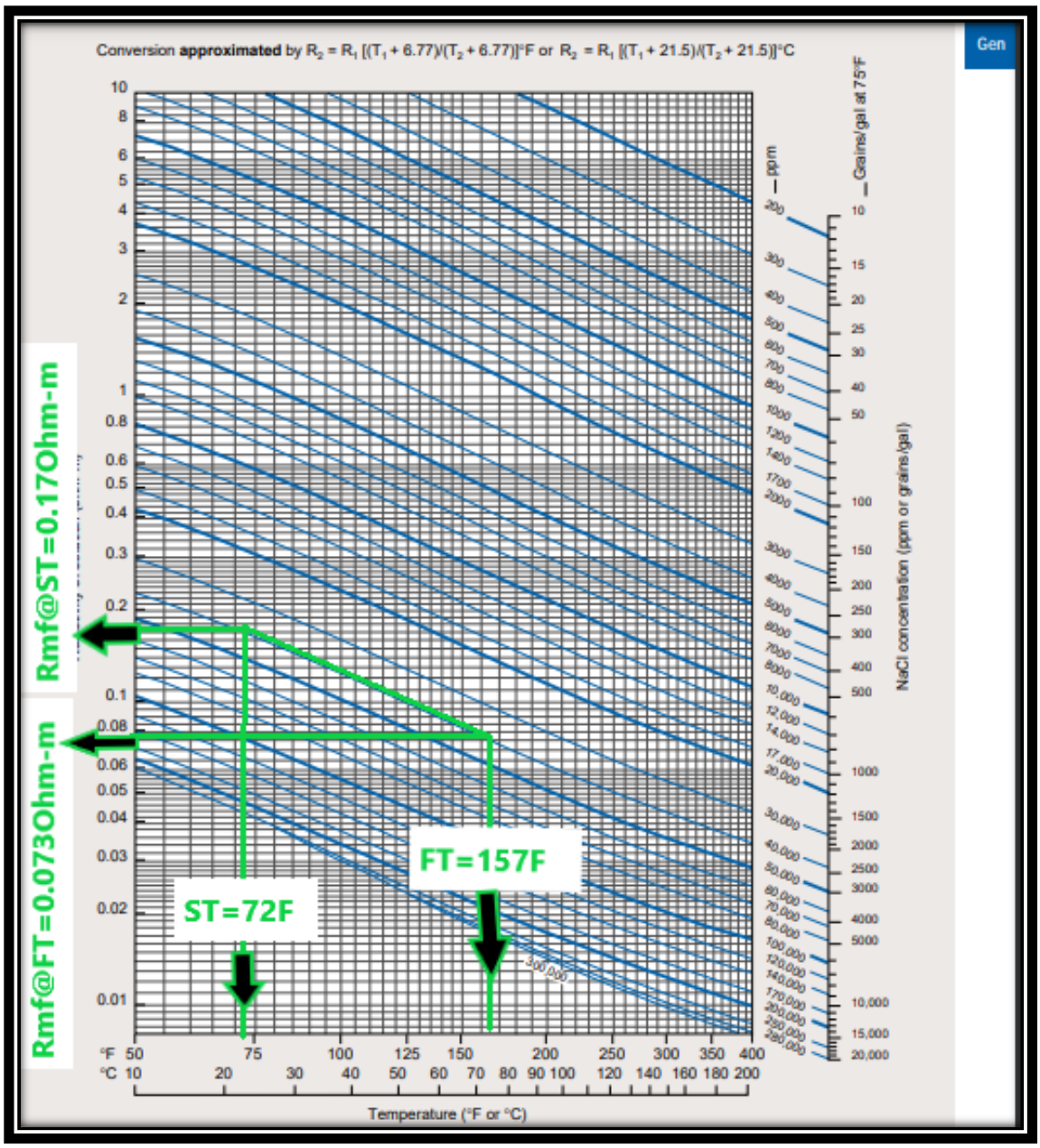

Figure 4.3. Gen-09 Chart of Sakessar Limestone.

In step four, Rmf at FT (resistivity of mud filtrate at formation temperature) is converted into Rmf at eq (resistivity of mud filtrate at equilibrium) with the help of SP-2 chart.

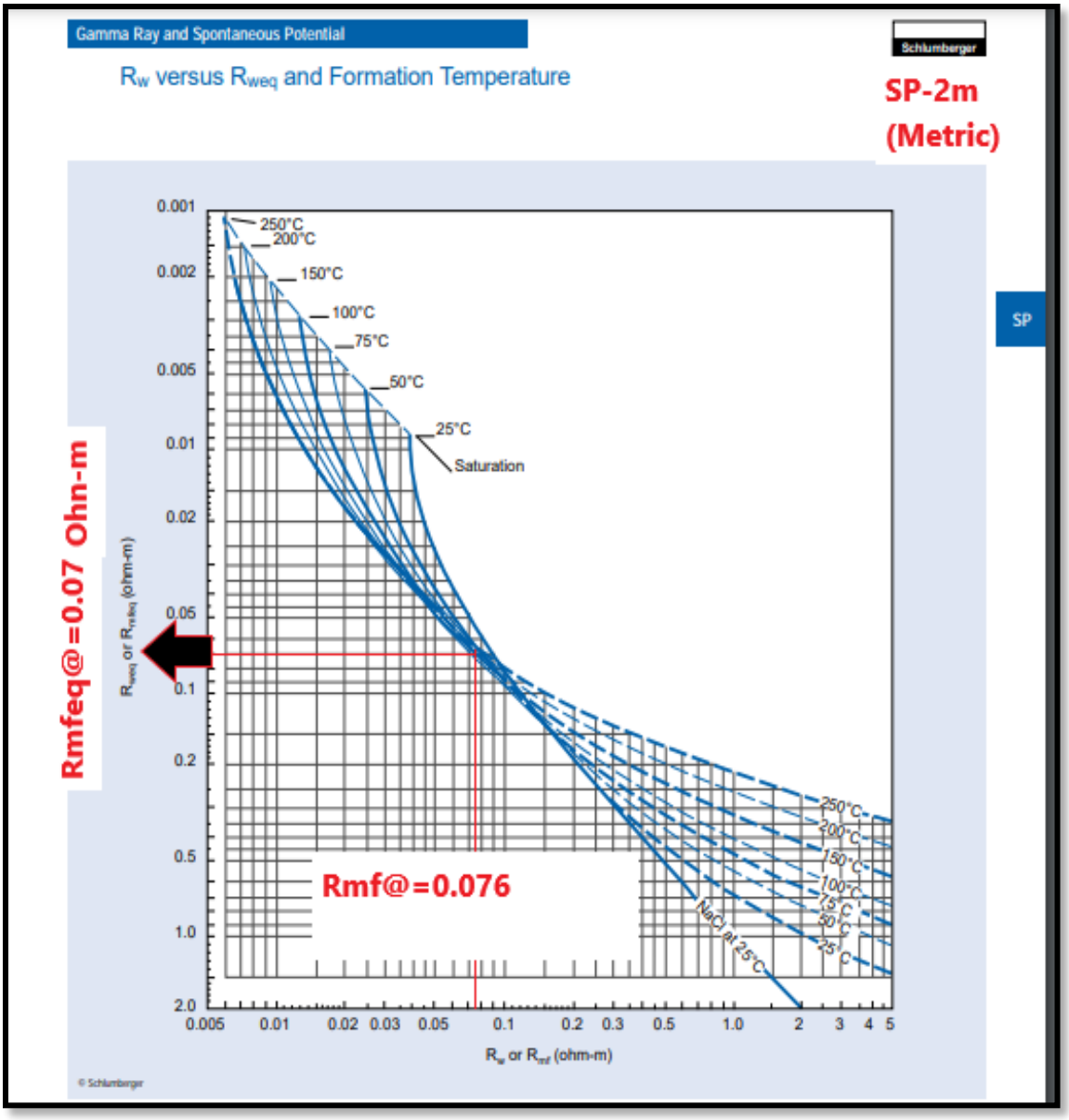

Figure 4.4. Rmf(eq) of Chorgali Formation.

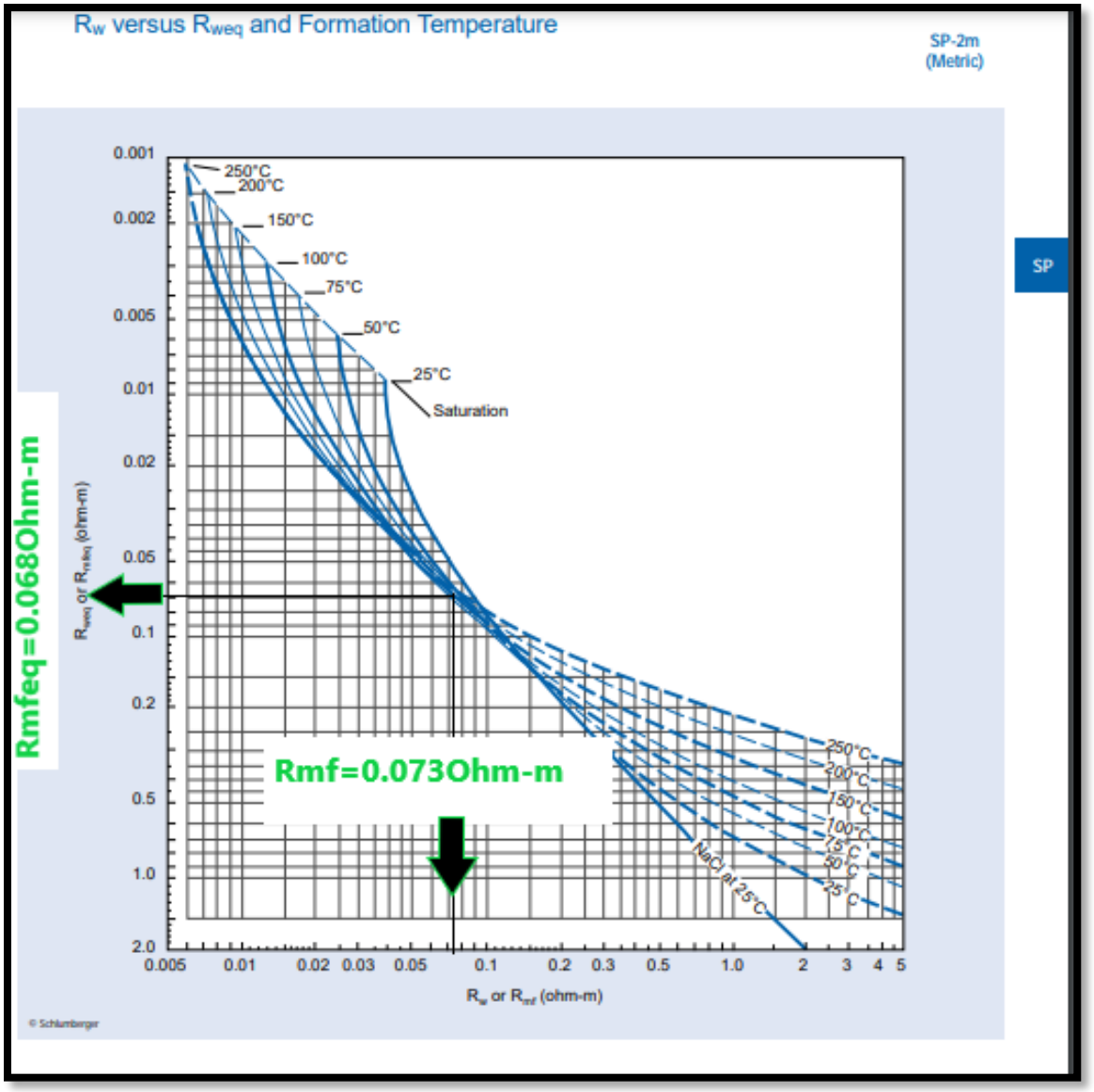

Figure 4.5. Rmf(eq) of Sakessar Limestone.

In fifth step, using the SP log value we calculate the SSP value which is-26 for Chorgali Formation and +14 for Sakessar Limestone. In the sixth step, the values of Rmfeq, SSP and Formation temp are plotted in SP-1 chart for both the formations and a straight line was passed from Rmf at equilibrium that gave the value of Rw at equilibrium.

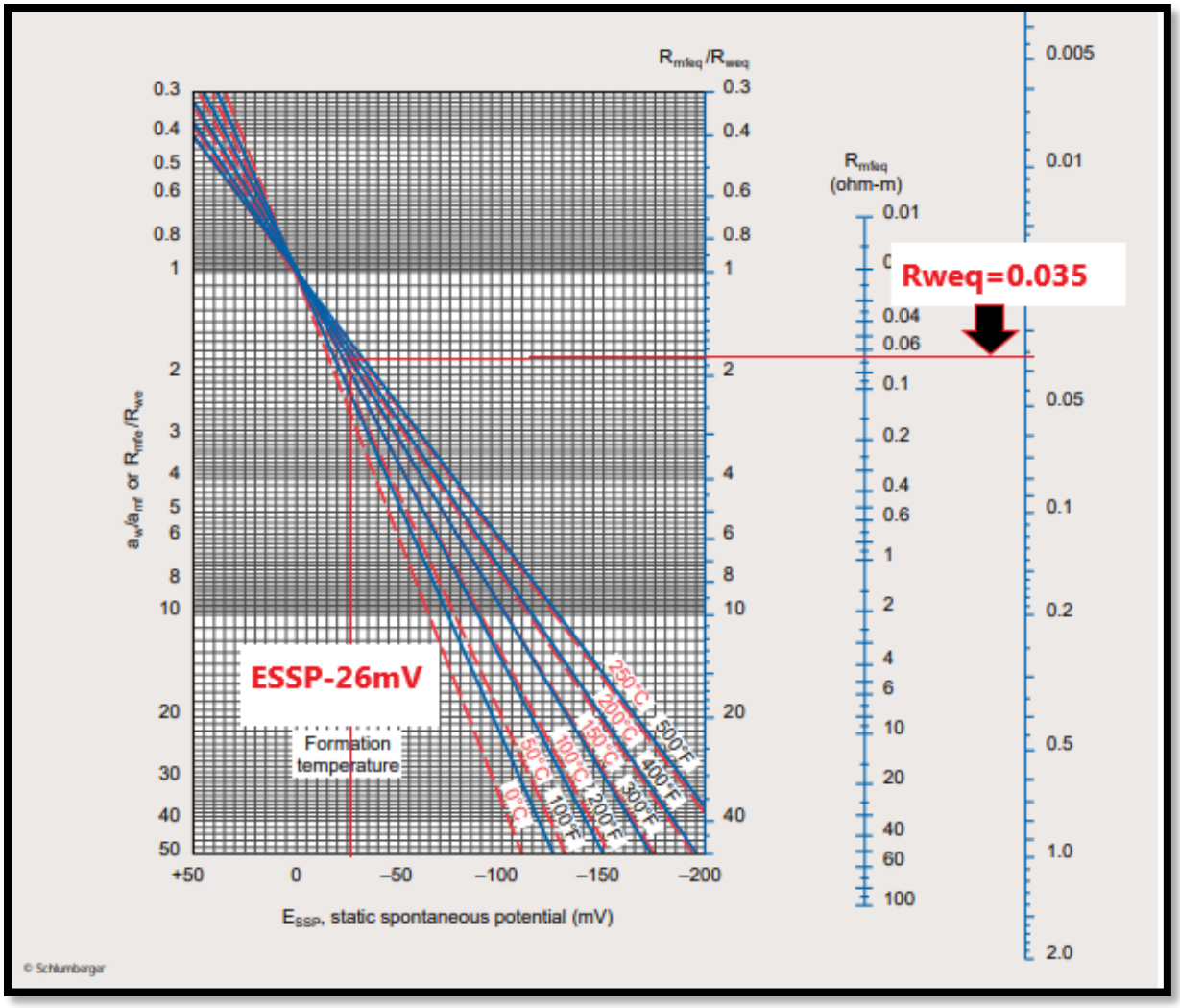

Figure 4.6. SP-01 Chart for Chorgali Formation.

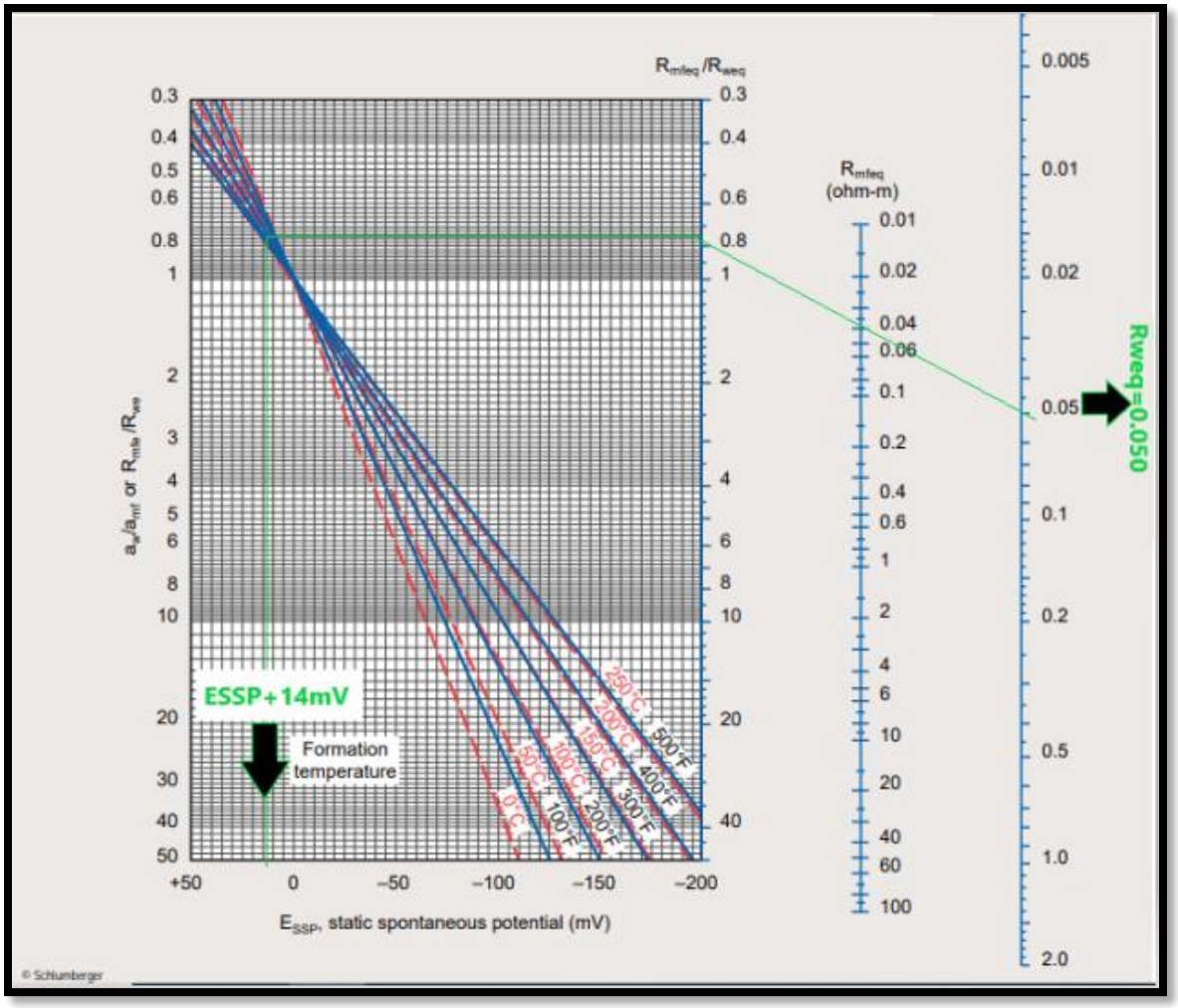

Figure 4.7. SP-01 chart for Sakessar Limestone.

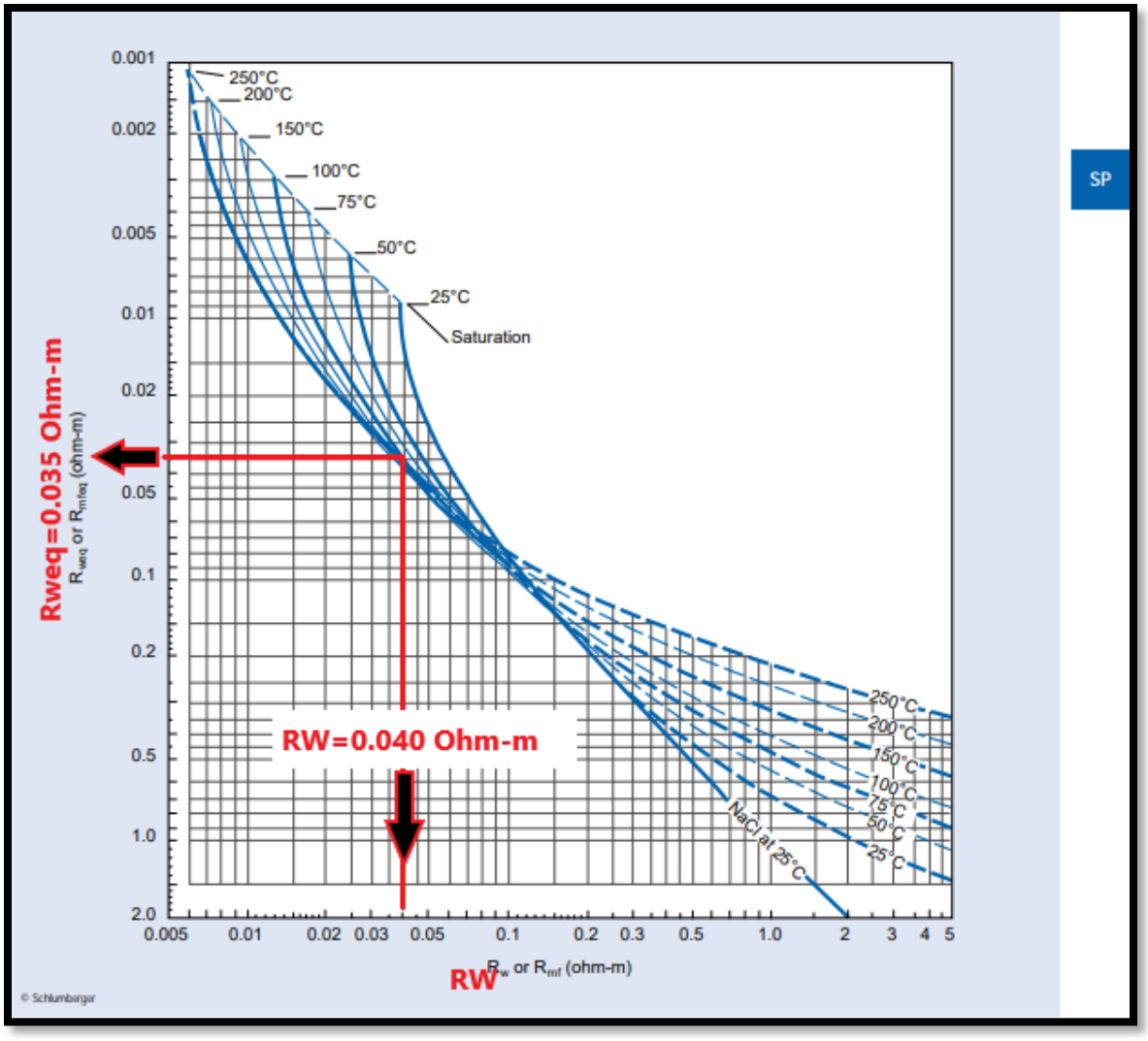

Figure 4.8. Sp-02 chart showing Rw for Chorgali Formation.

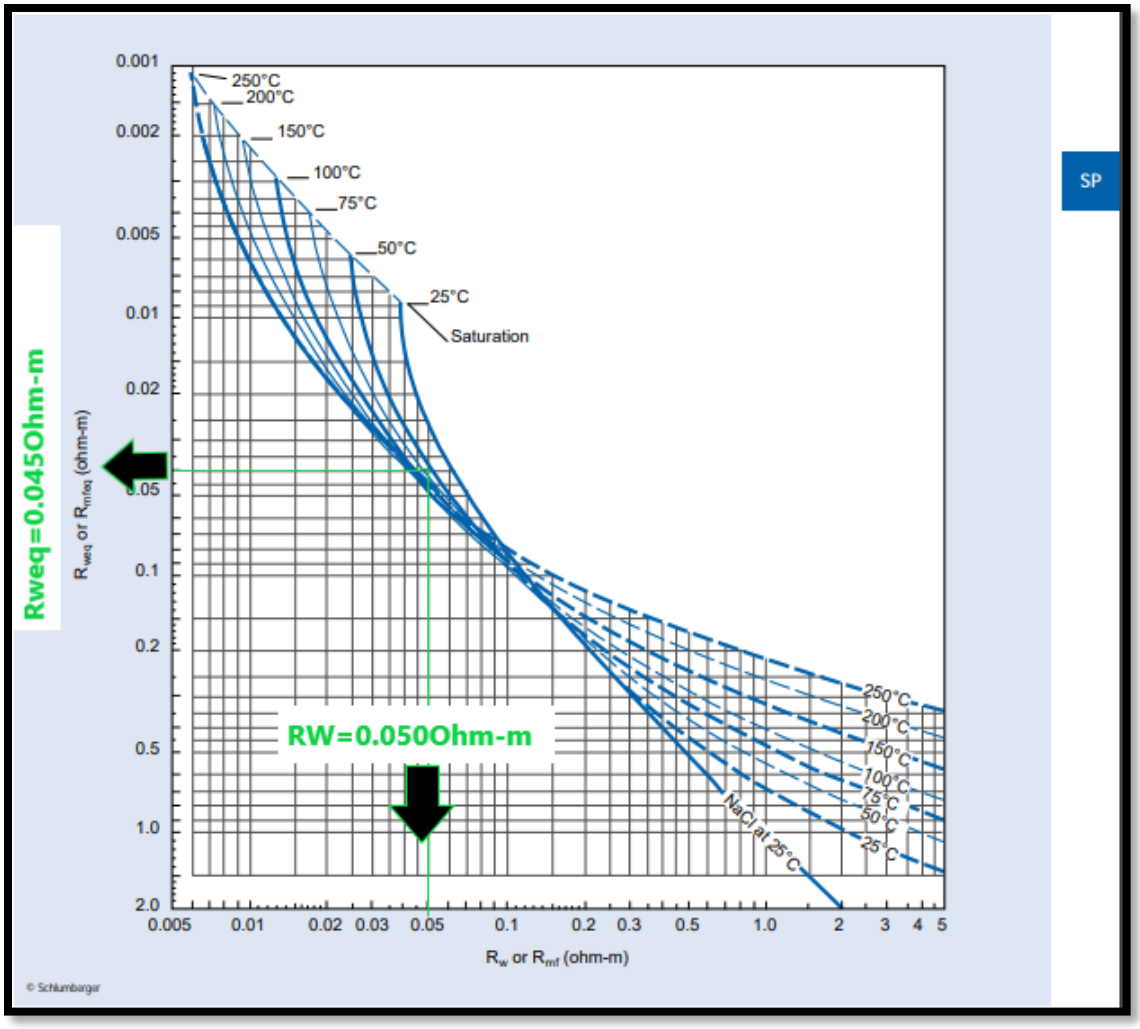

Figure 4.9. SP-02 chart using Rw for Sakessar Limestone.

Using the values Rweq plotted on the Sp-01 chart, we find the Resistivity of water Rw.

Table 4.4 Rw Calculation for both Chorgali Formation and Sakessar Limestone.

Chorgali Formation	**Sakessar Limestone**
Formation temperature= 155^{o}F	Formation temperature=157^{o}F
R_{mf} at formation temperature=0.076 ohm-m	R_{mf} at Formation temperature= 0.073 ohm-m
R_{mf} eq=0.07ohm-m	R_{mf} eq= 0.068 ohm-m
Rw at equivalent= 0.035 ohm-m	Rw at equivalent=0.045 ohm-m
Rw=0.040 ohm-m	Rw=0.050 ohm-m

4.6.5 Water saturation (S_w)

Water saturation indicates the presence of Hydrocarbon in the reservoir. The water saturation is calculated using Archie's equation which is given below

$$S_w = \sqrt{\left(\frac{Rw}{Rt}\right) * \left(\frac{1}{\emptyset_e^2}\right)} \qquad (4.8)$$

Here, S_w = Water saturation, R_w= Resistivity of water, R_t = True resistivity, Φ_e = Effective porosity

4.6.6 Saturation of hydrocarbon (S_h)

Hydrocarbon saturation gives the percentage of pore fraction having hydrocarbons. Saturation of hydrocarbons is calculated by the following formula

$$S_h = 1 - S_w \qquad (4.9)$$

Here, S_h = Saturation of hydrocarbon, S_w = Saturation of water

4.6.7 Limitation of our data

Zone of interest was not present in Sakesar Limestone given log data.

4.7 Interpretation of log data

Interpretation for reservoir in Balkassar Oxy-01 for Chorgali Formation and Sakessar Limestone are evaluated based on its porosities, saturation of fluids and shale content. These values are put into Excel sheet which in are used to create graphs.

4.7.1 Interpretation analysis of Chorgali Formation

Figure 4.7 shows the variations in volume of shale and volume of clean of Chorgali Formation with depth. The value of volume of shale (V_{sh}) ranges from 9.67 % to 45.25 % with the average value of 24.5%. The volume of clean (V_{clean}) ranges from 17.75 % to 90.32 % with the average value of 71.77 %.

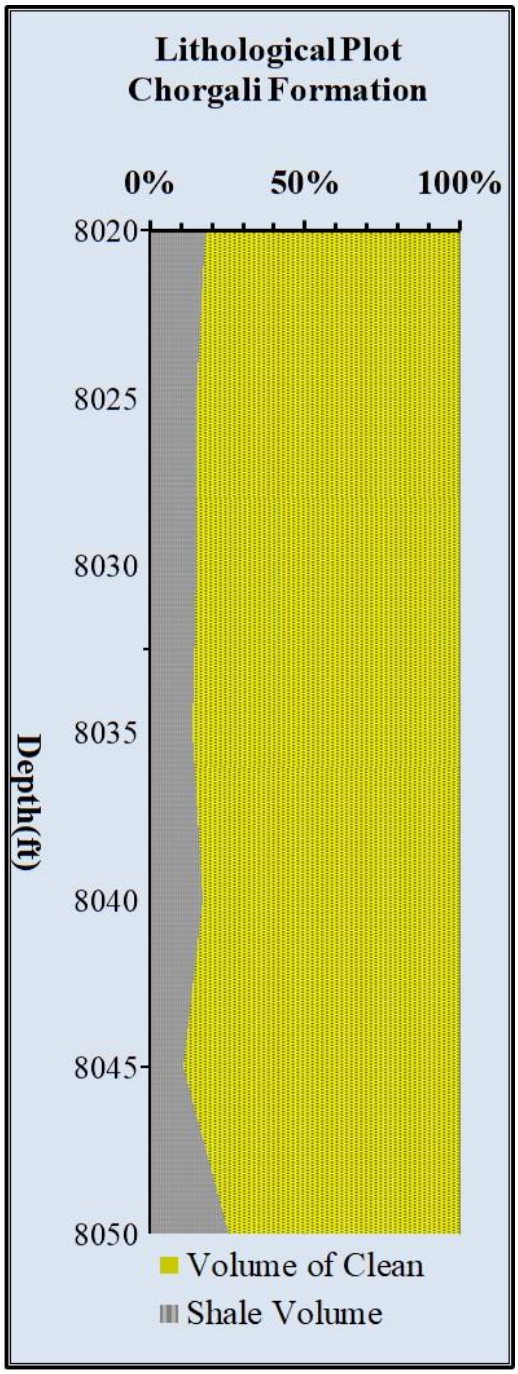

Figure 4.10. Graph showing variation in volume of shale and clean of Chorgali Formation with depth.

The percentage of average porosity in Chorgali Formation ranges from 11.407 to 13.20% and with an average value of 12.74%. The range of effective porosity ranges from 9.87% to 11.21% with an average value of 10.63%. The interpretation is concluded that

average porosity increases at depths where the volume of shale increases and show an appreciable separation of Average and Effective porosity at a depth of 8030 to 8040ft. When the volume of shale increases, the average and effective porosity decreases because shale is considered as a dirty lithology having large pore spaces, but poor connectivity and the shale chokes the pore spaces.

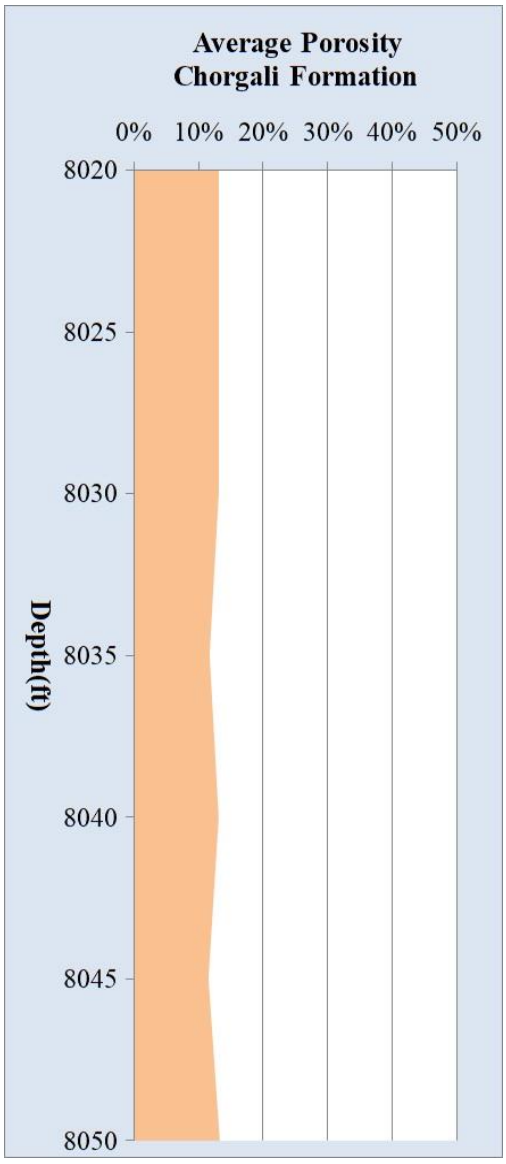

Figure 4.11 Graph showing variation in APHI value of Chorgali Formation with depth.

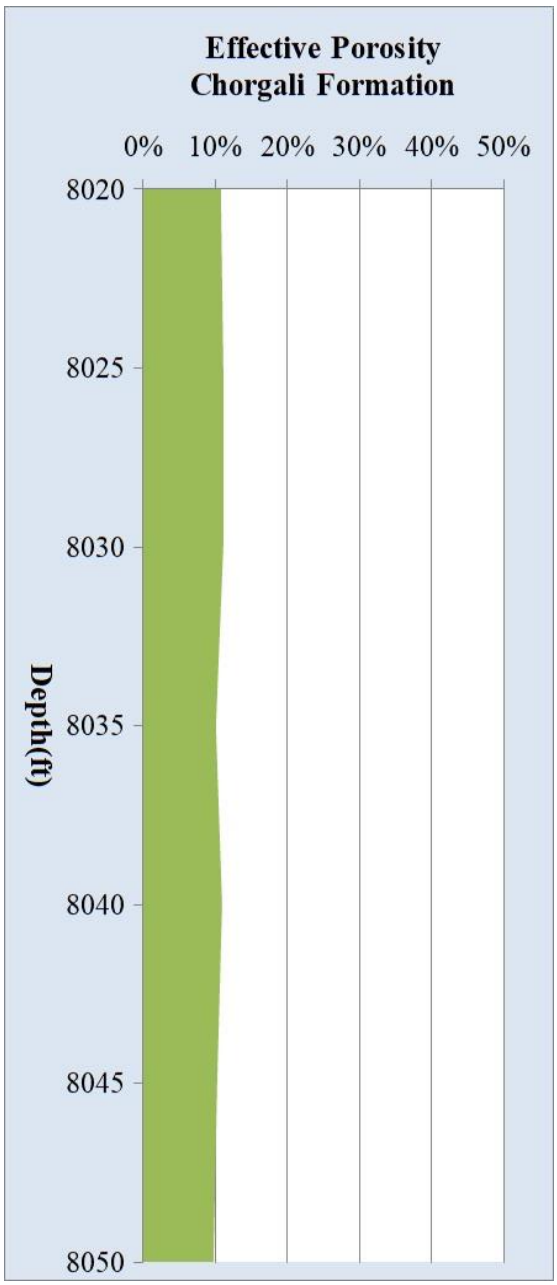

Figure 4.12. Graph showing variation in EPHI of Chorgali Formation with respect to depth.

The Chorgali Formation demonstrates variations of Sh and Sw with depths. The saturation of water ranges from 6.70% to 100% having an average value of 37.70%. The saturation of hydrocarbon ranges from 0 to 93.20% having an average value of 62.29%.

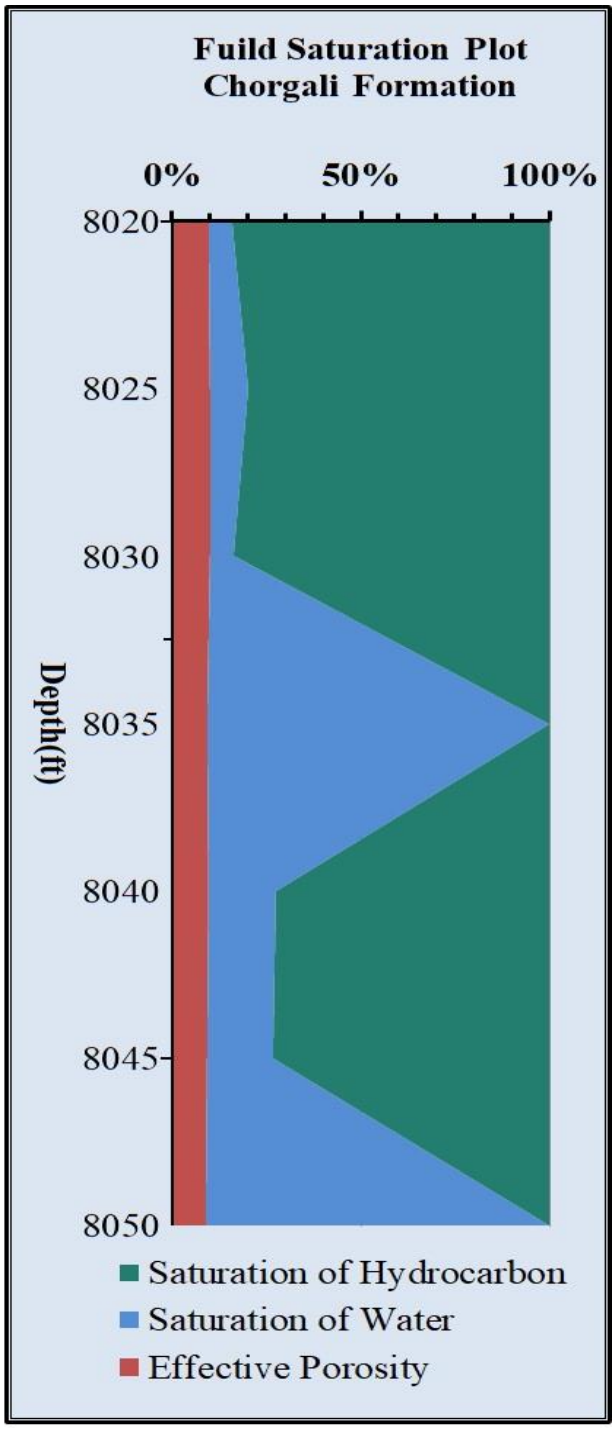

Figure 4.13. Graph showing variation of Sh% and Sw% and EPHI with depth of Chorgali Formation.

4.7.2 Interpretation analysis of Sakessar Limestone

Figure 4.16 shows the variations in volume of shale and volume of clean of Sakessar limestone with depth. The value of volume of shale (V_{sh}) ranges from 5.172 % to 52.38 % with the average value of 16.67%. The volume of clean (V_{clean}) ranges from 72 % to 100 % with the average value of 73.710 %.

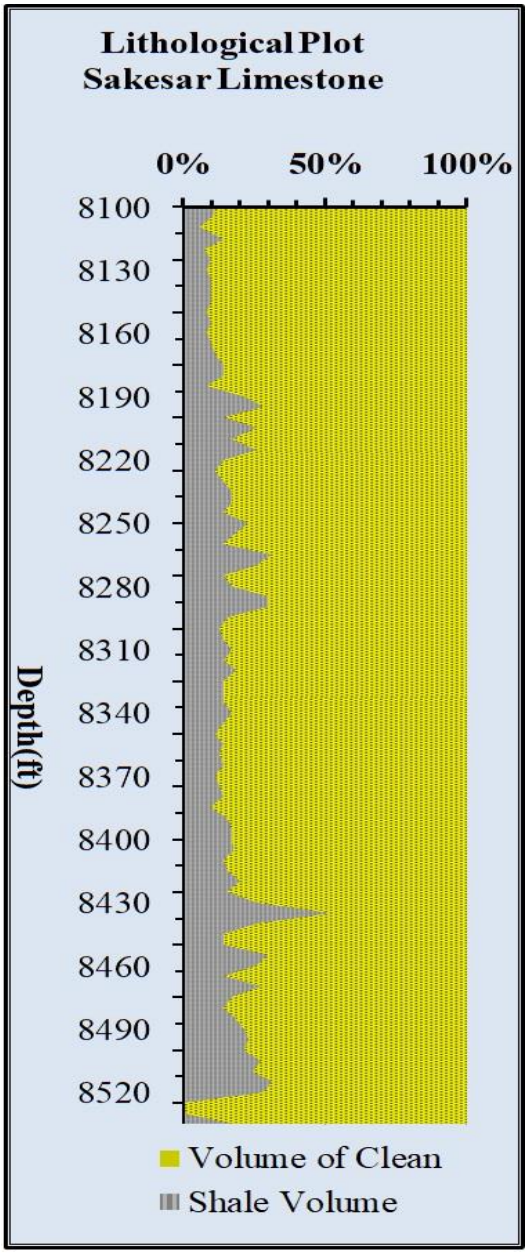

Figure 4.14 Graph showing variation in volume of shale and clean of Sakessar Limestone with depth.

The Sakessar limestone demonstrates variations of Sh and Sw with depths. The saturation of water ranges from 10.102% to 100% having an average value of 68.37%. The saturation of hydrocarbon ranges from 0 to 89% having an average value of 30.317%.

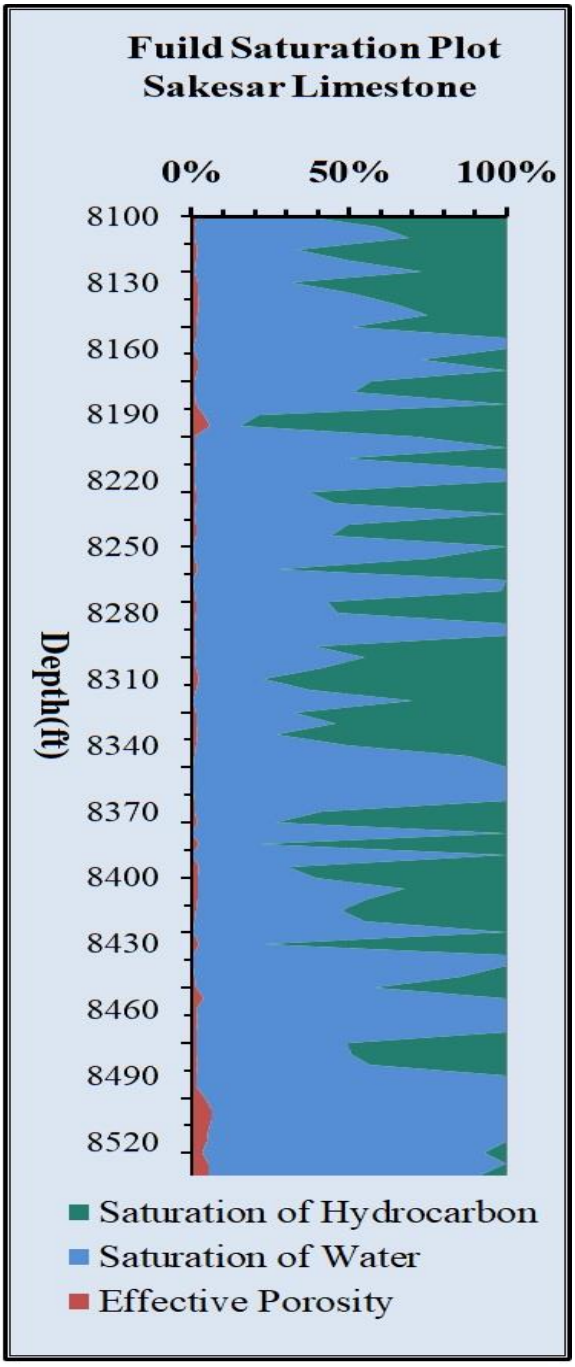

Figure 4.15 Graph showing variation of Sh% and Sw% with depth of Sakessar Limestone

The percentage of average porosity in Sakessar limestone ranges from 0.89% to 85% and with an average value of 12.4001%. The range of effective porosity ranges from 0.062% to 5.48% with an average value of 1.809%. The interpretation is concluded that average porosity increases at depths where the volume of shale decreases. When the volume of shale increases, the average and effective porosity decreases because shale is considered as a dirty lithology having large pore spaces, but poor connectivity and the shale chokes the pore spaces.

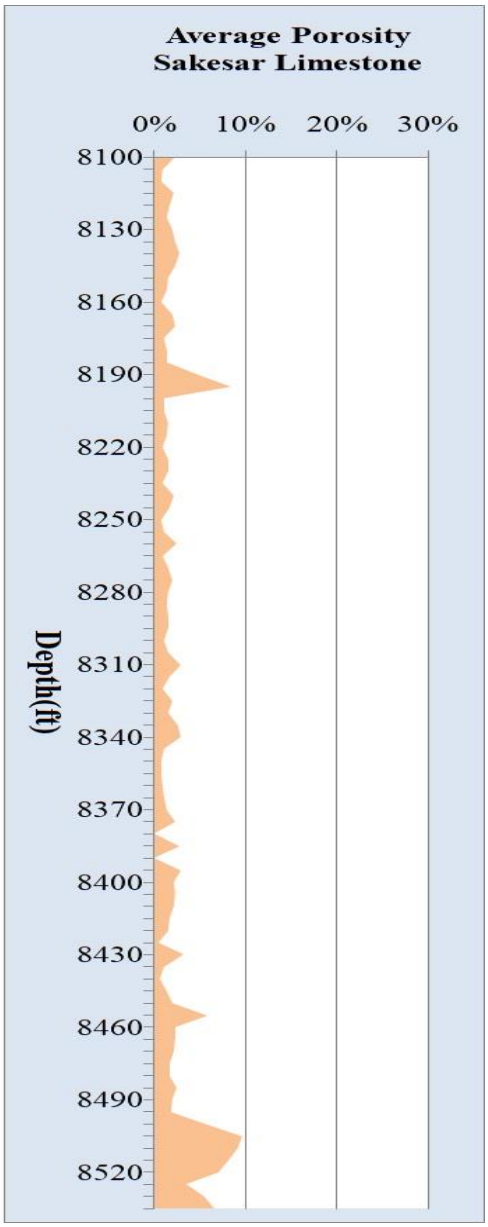

Figure 4.16. Graph showing variation of APHI of Sakessar Limestone depth.

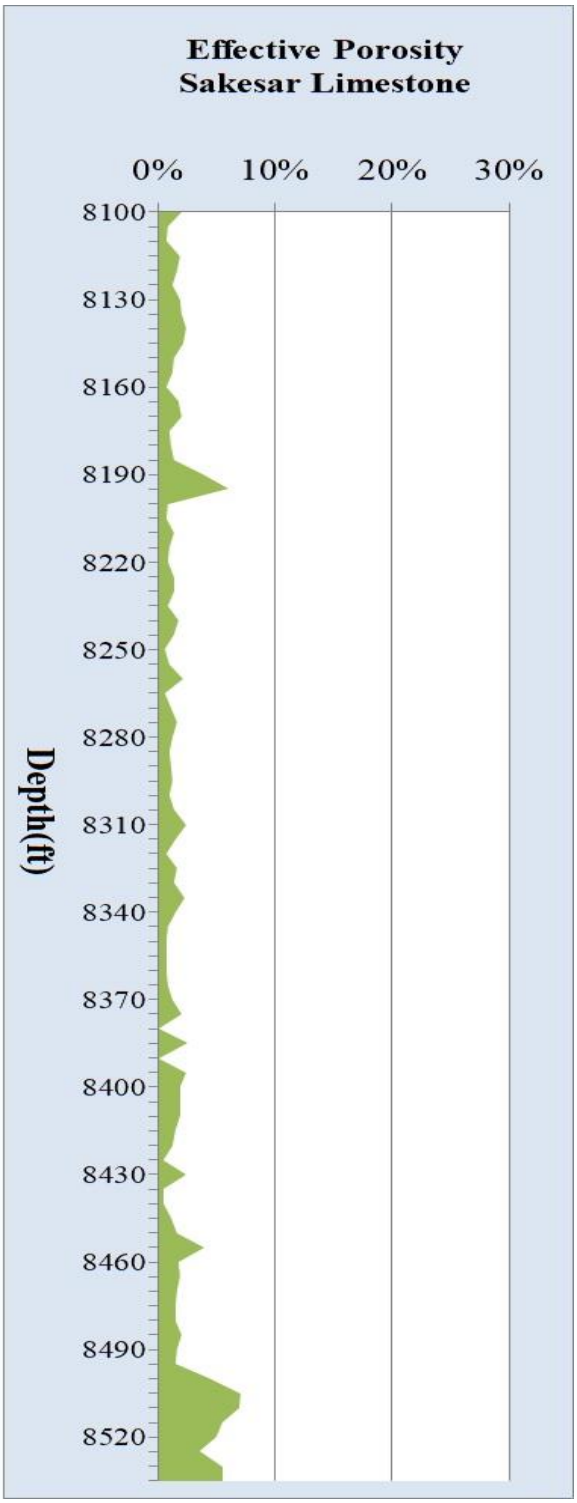

Figure 4.17. Graph showing variation in EPHI of Sakessar Limestone with depth.

CONCLUSIONS

1. Seismic interpretation delineates the pop-up anticlinal structure thrusted with two thrust faults dipping towards north and south directions which is a positive geometry for hydrocarbon entrapment. The time and depth contour maps confirms the presence of pop-up structure making a two-way dip closure.

2. Petrophysical analysis depicted only one zone in Chorgali Formation with sufficient hydrocarbon saturation (62.29%.) and effective porosity (10.63%.) proving it to be a good reservoir (30 feet thickness).

REFERENCES

Aamir, M. and Siddiqui, M.M., 2006. Interpretation and visualization of thrust sheets in a triangle zone in eastern Potwar, Pakistan. *The Leading Edge*, *25*(1), pp.24-37.

Abid, M., Riaz, M., Shah, M., Zafar, T., & Malik, A. (2019). Structural interpretation and reservoir characterization of the Missa Keswal area, upper Indus basin, Pakistan. Bollettino di Geofisica Teorica ed Applicata, 60(3).

Archie, G. E. (1950). Introduction to petrophysics of reservoir rocks. AAPG bulletin, 34(5), 943-961.

Badley, M. E., & Gibson, B. (1987). Practical Seismic Interpretation by Michael E. Badley.

Bender, Fk & Raza, ha (eds) 1995. geology of pakistan. x+ 414 pp.+ maps in box. beitrage zur regionalen geologie der erde, band 25. berlin, stuttgart: gebrüder borntraeger

Dobrin, M.B. and Savit, C.H., 1988. Introduction to Geophysical Prospecting, McGraw Hill International edition, geology series.

Duncan, R.A., and Pyle, D.G., 1988. Rapid eruption of the Deccan flood basalts at the Cretaceous/Tertiary boundary. Nature, 333(6176), pp.841-843.

Ghazi, S., Ali, S. H., Sahraeyan, M., & Hanif, T. (2015). An overview of tectonosedimentary framework of the Salt Range, northwestern Himalayan fold and thrust belt, Pakistan. Arabian Journal of Geosciences, 8(3), 1635-1651.

Hasany, S.T. and Saleem, U., 2012. An integrated subsurface geological and engineering study of Meyal Field, Potwar Plateau, Pakistan. Search and Discovery Article, 20151, pp.1-41.

Iqbal, M., and Ali, S.M., 2001. Correlation of structural lineaments with oil discoveries in Potwar sub-basin, Pakistan. Pakistan Journal of Hydrocarbon Research, 12, pp.73-80.

Ishimwe, D., 2014. PETROLEUM SYSTEMS AND ELEMENTS OF PETROLEUM GEOLOGY. SPE CONNECT.

Jadoon, Waqar AK, B. A. Shami, and Iftikhar A. Abbasi. "Fracture analysis of Khaur anticline and its implications on subsurface fracture system." PAPG-SPE AnnualTechnical Conference and Oil Show. 2003.

John Milsom, Asger Eriksen (2011), Field Geophysics, Fourth Edition. Environmental and Engineering Geoscience; 19 (2): 205–206.

Joncheray, B. and Rainon, E., 1978. Stratigraphic Interpretation of Seismic Data. The Log Analyst, 19(06).

Kadri, I. B. (1995). Petroleum Geology of Pakistan: Pakistan Petroleum Limited. Karachi, Pakistan.

Kazmi, A. H., & Jan, M. Q. (1997). Geology and tectonics of Pakistan. Graphic publishers.

Khan, M.A., Ahmad, R., Raza, H.A. and Kemal, A., 1986.Geology of petroleum in Kohat-Potwar Depression, Pakistan. AAPG Bull., 70, 396-414

Lillie, R.J., Johnson, G.D., Yousuf, M., Zamin, A.S.H. and Yeats, R.S., 1987. Structural development within the Himalayan foreland fold-and-thrust belt of Pakistan.

Patriat, P. and Achache, J., 1984. India–Eurasia collision chronology has implications for crustal shortening and driving mechanism of plates. Nature, 311(5987), pp.615-621.

Rider, M.H., 1986. The geological interpretation of well logs.

Sarasty, J.J. and Stewart, R.R., 2003. Analysis of well-log data from the White Rose oilfield, offshore Newfoundland. CREWES Res Rep, 15, pp.1-16.

Schlumberger Limited. (1972). Schlumberger Log Interpretation: Principles (Vol. 1). Schlumberger Limited

Sercombe, W.J., Pivnik, D.A., Wilson, W.P., Albertin, M.L., Beck, R.A. and Stratton, M.A., 1998. Wrench faulting in the northern Pakistan foreland. AAPG bulletin, 82(11), pp.2003-2030.

Shakir, U., Abbas, M., Ahmad, W., Mahmood, M.F., Hussain, M., Anwar, M., Sikandar, U. and Naseem, T., 2020. Hydrocarbon Reservoir Evaluation and Fault Seal Analysis of Balkassar Area, Potwar Sub Basin, Pakistan. The Nucleus, 56(3), pp.96-104

Tiab, D., & Donaldson, C. (2004). Petrophysics Second Edition–Theory and Practice of Measuring Reservoir Rock and Fluid Transport Properties

Warwick, P.D., 2007. Overview of the geography, geology and structure of the Potwar regional framework assessment project study area, northern Pakistan. In: Warwick, P.D., Wardlaw, B.R. eds., Regional Studies of the Potwar Plateau Area, northern Pakistan. US Geological Survey Bulletin, 2078

Zaman, A.S. and Zahidi, S.A., 1996. Missa Keswal oil field Potwar, Pakistan, a failure turned into success. AAPG Bulletin, 5(CONF-960527-).